

Performance and design of full-width RHS X and T joints under brace axial tension and brace bending

Lan, Xiaoyi; Wardenier, Jaap; Packer, Jeffrey A.

DOI

[10.1016/j.tws.2022.110001](https://doi.org/10.1016/j.tws.2022.110001)

Publication date

2022

Document Version

Final published version

Published in

Thin-Walled Structures

Citation (APA)

Lan, X., Wardenier, J., & Packer, J. A. (2022). Performance and design of full-width RHS X and T joints under brace axial tension and brace bending. *Thin-Walled Structures*, 181, Article 110001. <https://doi.org/10.1016/j.tws.2022.110001>

Important note

To cite this publication, please use the final published version (if applicable). Please check the document version above.

Copyright

Other than for strictly personal use, it is not permitted to download, forward or distribute the text or part of it, without the consent of the author(s) and/or copyright holder(s), unless the work is under an open content license such as Creative Commons.

Takedown policy

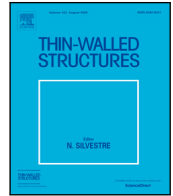
Please contact us and provide details if you believe this document breaches copyrights. We will remove access to the work immediately and investigate your claim.

Green Open Access added to TU Delft Institutional Repository

'You share, we take care!' - Taverne project

<https://www.openaccess.nl/en/you-share-we-take-care>

Otherwise as indicated in the copyright section: the publisher is the copyright holder of this work and the author uses the Dutch legislation to make this work public.



Full length article

Performance and design of full-width RHS X and T joints under brace axial tension and brace bending

Xiaoyi Lan^{a,*}, Jaap Wardenier^b, Jeffrey A. Packer^c^a School of Civil Engineering and Transportation, South China University of Technology, Guangzhou, China^b Department of Engineering Structures, Delft University of Technology, The Netherlands^c Department of Civil & Mineral Engineering, University of Toronto, Canada

ARTICLE INFO

Keywords:

X joints
T joints
Rectangular hollow section
Design rules
Chord sidewall failure
Brace failure
Brace axial tension
Brace bending

ABSTRACT

Within the research framework for updating the international design standard ISO 14346 for hollow section joints, this study examines brace failure and chord sidewall failure in full-width rectangular hollow section (RHS) X and T joints under brace axial tension, brace in-plane bending and brace out-of-plane bending. The codified design rules for full-width RHS joints are reviewed, with their limitations highlighted. Design resistance equations for brace failure, based on the modified effective width method, and also for chord sidewall failure, using the modified bearing-buckling method and the Lan-Kuhn method, are then proposed. Up-to-date experimental and numerical results are collated from the literature, which cover a wide range of geometrical parameters, steel grades ranging from S235 to S960, varying weld details, and loading cases of brace axial tension, brace in-plane bending and brace out-of-plane bending. The compiled results are adopted to evaluate the performance of full-width RHS joints and to assess suitability of the proposed design resistance equations. It is shown that weld details can significantly affect the deformation capacity and static strengths of full-width RHS joints. The proposed design resistance equations yield conservative and reliable strength predictions for full-width RHS joints. Welding guidance and user-friendly design rules, in which an extension to include Class 3 cross-sections is included, are suggested for full-width RHS X and T joints.

1. Introduction

Rectangular hollow sections (RHS) combine evident structural advantages, particularly for members loaded in compression or torsion, with an architecturally attractive shape, and allow easy connections to the flat face. This has resulted in widespread applications of RHS in buildings, bridges, towers, cranes and sculptures, for example. The zone, where one or more intersecting brace members are welded to the through RHS chord member, is called a welded RHS joint. Failure of one or more RHS joints could trigger the collapse of an entire structure, highlighting the significance of performance of RHS joints on the structural integrity, and this necessitates suitable design rules for RHS joints.

The configuration and notation for RHS-to-RHS X and T joints are illustrated in Fig. 1. Brace failure and chord sidewall failure are the two representative failure modes in full-width RHS X and T joints, having a brace-to-chord width ratio (β) of 1.0, under brace axial tension, brace in-plane bending and brace out-of-plane bending. Experimental investigations on RHS joints date back to the 1960s by tube suppliers Stewarts and Lloyds in the UK [1] and Mannesmann in Germany [2], with some initial test programs, for example, at the

University of Sheffield [3]. In the 1970s, the international organisation of tube suppliers CIDECT sponsored several research programs, and those including full-width RHS X and T joints were reported by, among others, Wardenier and de Koning [4], Barentse [5], Davies et al. [6] and Mang et al. [7]. Using a conservative lower-bound of the test results of full-width X and T joints, which were made of hot-formed hollow sections and cross-sections fabricated from two cold-formed channel sections, Wardenier and Davies [8] and Wardenier [9] proposed a design-oriented brace effective width method for brace failure, and a bearing-buckling model for chord sidewall failure. These two design models have been adopted by design codes and guides, including EN 1993-1-8 [10], ISO 14346 [11], CIDECT design guide No. 3 [12,13] and the IIW recommendations [14–16].

The behaviour and design for limit states of brace failure and chord sidewall failure in full-width RHS joints have been examined more extensively after the early 1980s. Experimental and numerical investigations on mild steel full-width RHS X and T joints have been conducted by, among others, Kanatani et al. [17], Tabuchi et al. [18], Mang et al. [19], Packer [20], Yu [21] and Björk [22]. To extend the scope of RHS X and T joints to steel grades higher than S355, investigations

* Corresponding author.

E-mail address: lanxiaoyi@scut.edu.cn (X. Lan).

Nomenclature

a	Weld throat thickness
A_0	Chord cross-sectional area
A_1	Brace cross-sectional area
A_e	Brace cross-sectional effective area
b_0	Chord width
b_1	Brace width
b_e	Brace effective width
C_{f0}	Chord material factor
C_{f1}	Brace material factor
E	Elastic modulus
f_k	Buckling stress of chord sidewall
f_{y0}	Chord yield stress
f_{y1}	Brace yield stress
f_{u0}	Chord ultimate stress
f_{u1}	Brace ultimate stress
h_0	Chord depth
h_1	Brace depth
t_0	Chord wall thickness
t_1	Brace wall thickness
θ_1	Angle between brace and chord
$M_{0,Ed}$	Bending moment acting in the chord
$M_{el,0,Rd}$	Design chord elastic moment resistance
$M_{pl,0,Rd}$	Design chord plastic moment resistance
$M_{ip,1,Rd}$	Design in-plane moment resistance of a joint
$M_{ip,1u}$	Actual in-plane moment capacity of a joint
$M_{ip,BF}$	Predicted in-plane moment capacity for brace failure
$M_{ip,CSF}$	Predicted in-plane moment capacity for chord sidewall failure
$M_{ip,Pred}$	Predicted in-plane moment capacity of a joint
$M_{ip,pl}$	Brace in-plane plastic moment capacity
$M_{op,1,Rd}$	Design out-of-plane moment resistance of a joint
$M_{op,1u}$	Actual out-of-plane moment capacity of a joint
$M_{op,BF}$	Predicted out-of-plane moment capacity for brace failure
$M_{op,CSF}$	Predicted out-of-plane moment capacity for chord sidewall failure
$M_{op,Pred}$	Predicted out-of-plane moment capacity of a joint
$M_{op,pl}$	Brace out-of-plane plastic moment capacity
N_{1u}	Actual axial load capacity of a joint
$N_{1,Rd}$	Design axial resistance of a joint
$N_{0,Ed}$	Axial load acting in the chord
$N_{pl,0,Rd}$	Design chord plastic axial resistance $A_0 f_{y0}$
N_{BF}	Predicted axial load capacity for brace failure
N_{CSF}	Predicted axial load capacity for chord sidewall failure

N_{Pred}	Predicted axial load capacity
N_{y1}	Brace cross-sectional yield load $A_1 f_{y1}$
n	Chord stress ratio
Q_f	Chord stress function
$W_{el,0}$	Chord cross-sectional elastic modulus
$W_{el,1}$	Brace cross-sectional elastic modulus
$W_{pl,0}$	Chord cross-sectional plastic modulus
$W_{pl,1}$	Brace cross-sectional plastic modulus
β	Brace-to-chord width ratio b_1/b_0
2γ	Chord width-to-thickness ratio b_0/t_0
λ_C	Codified chord sidewall slenderness
$\lambda_{0.5}$	Chord sidewall slenderness equal to $0.5\lambda_C$
χ_C	Buckling reduction coefficient for λ_C
$\chi_{0.5}$	Buckling reduction coefficient for $\lambda_{0.5}$
ϕ	Resistance factor for a joint

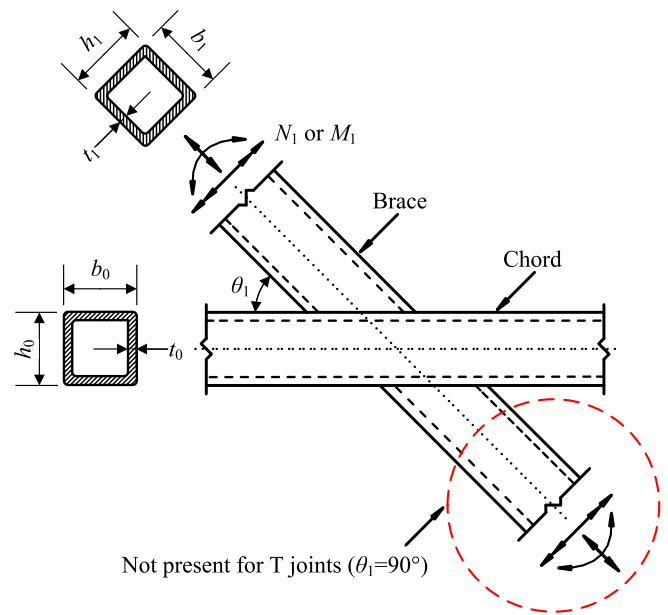


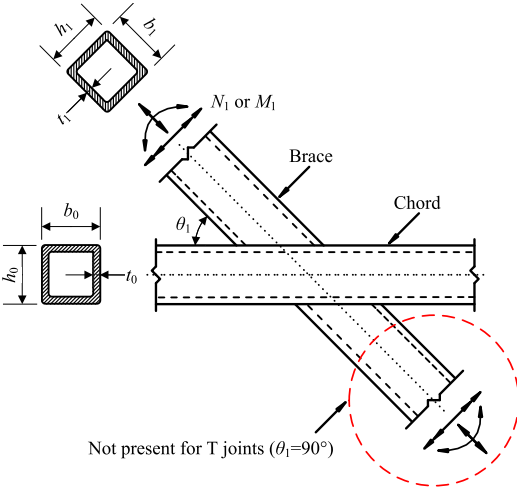
Fig. 1. The configuration and notation for RHS-to-RHS X and T joints.

is shown that the codified bearing–buckling method for chord sidewall failure in full-width RHS joints under brace axial compression is considerably conservative if the joints are adequately supported out-of-plane. In order to address this issue, various analytical models have been proposed, e.g., the four-hinge yield line model by Yu [21], the modified column model by Kuhn et al. [35], and the plate buckling models by Lan et al. [33,34] and Becque and Cheng [36]. Wardenier et al. [37] and Lan et al. [38] examined the representative analytical models against the reported test and numerical results in the literature. Two alternative design methods, i.e., a modified bearing–buckling method and a so-called simplified Lan–Kuhn method, for chord sidewall failure in full-width RHS joints under brace axial compression, using steel grades up to S960, were proposed. These two design methods and resulting user-friendly design rules have been adopted by IIV Sub-commission XV-E, which is the drafting committee for the update of ISO 14346 [11]. However, a comprehensive evaluation of the suitability of these design methods for brace failure and chord sidewall failure in full-width RHS joints under brace tension and bending loading, in particular for high-strength steel, remains absent.

As part of the research programme to update ISO 14346 [11], this study aims to investigate brace failure and chord sidewall failure in

have been covered in Björk and Saastamoinen [23], Tuominen and Björk [24], Feldmann et al. [25], Becque and Wilkinson [26], Kim et al. [27,28], Pandey and Young [29–32] and Lan et al. [33,34]. It

Table 1Codified design resistance equations for **brace failure** in RHS X and T joints [11,13,16].

Design resistance	Brace axial loading
	$N_{1,Rd} = C_{t1} f_{y1} t_1 (2h_1 + 2b_e - 4t_1)$
	Brace in-plane bending
	$M_{ip,1,Rd} = C_{t1} f_{y1} [W_{pl,1} - (b_1 - b_e)(h_1 - t_1)t_1]$
	Brace out-of-plane bending
	$M_{op,1,Rd} = C_{t1} f_{y1} [W_{pl,1} - 0.5t_1(b_1 - b_e)^2]$
	Parameters
	1. Brace effective width (b_e) is determined from: $b_e = \frac{10}{b_0/t_0} \frac{f_{y0} t_0}{f_{y1} t_1} b_1 \text{ but } \leq b_1$
	2. Brace material factor (C_{t1}) is taken as: $C_{t1} = 1.0$ for $f_{y1} \leq 355$ MPa and $C_{t1} = 0.9$ for $355 < f_{y1} \leq 460$ MPa
	3. Steel yield stress (f_y) for design shall be: $f_{y0} \leq 460$ MPa, $f_{y1} \leq 460$ MPa, $f_{y0} \leq 0.8f_{u0}$, $f_{y1} \leq 0.8f_{u1}$, $f_{y1} \leq f_{y0}$
	Validity ranges
	$b_1/t_1 \leq 40$, $h_1/t_1 \leq 40$, Class 1 or 2 cross-section for the brace and chord under compression stress; $0.5 \leq h_0/b_0 \leq 2.0$; $\theta_1 \geq 30^\circ$

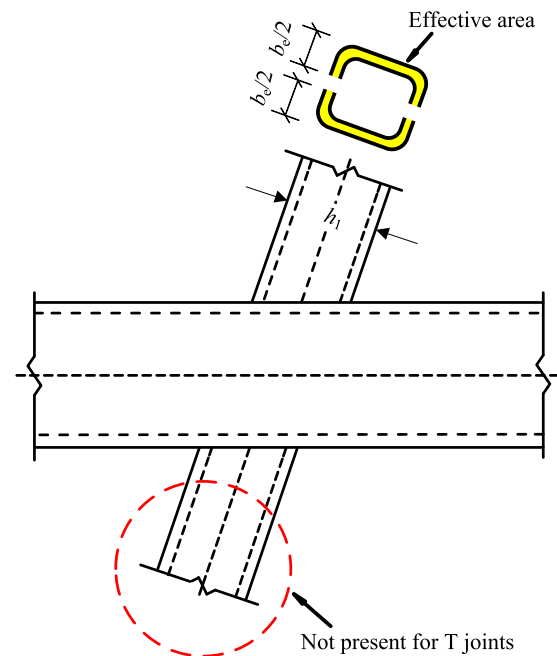
full-width RHS X and T joints under brace axial tension, brace in-plane bending and brace out-of-plane bending, which is a follow-up of Wardenier et al. [37] and Lan et al. [38] for brace axial compression. Design resistance equations for brace failure and chord sidewall failure in mild steel and high-strength steel RHS joints under brace axial tension and brace bending have been proposed, and these are assessed herein against results collated from the literature. Influences of geometrical parameters, steel grades, weld details and loading cases are discussed, and reliability of the proposed design resistance equations is verified by reliability analyses. Finally, welding guidance and user-friendly design rules are recommended for full-width RHS joints.

2. Current design rules

2.1. Codified design rules

Brace failure and chord sidewall failure are the two typical failure modes in full-width RHS joints under brace axial tension, brace in-plane bending and brace out-of-plane bending. In the case of brace failure (see Fig. 2), two brace sidewalls with a height (h_1) are fully effective. However, due to the non-uniform stiffness distribution at the connection with the chord face, the brace cross-walls with a width (b_1) have a non-uniform stress distribution which is simplified to be a brace effective width (b_e) at both cross-walls for design, resulting in a brace cross-sectional effective area of $A_e = (2h_1 + 2b_e - 4t_1)t_1$, if treated as a box section. In the cases of brace axial tension and brace bending (for Class 1 or 2 brace cross-sections), the joint resistance is related to the brace yield stress (f_{y1}). Table 1 shows the corresponding current design rules codified in ISO 14346 [11], CIDECT design guide No. 3 [13] and the IIW recommendations [16], for full-width RHS X and T joints using steel grades up to S460, which are based on the effective width method [8,9]. The brace and chord yield stresses (f_{y1} and f_{y0}) are limited to 0.8 times the brace and chord ultimate stresses (f_{u1} and f_{u0}), respectively, to provide, similar to mild steel, an adequate safety margin on the ultimate stress, which is low for high-strength steel. It is noted that the codified equation of brace cross-sectional effective area (A_e), assuming a sharp tube corner, over-estimates the actual brace effective area for cold-formed hollow sections, having large corner radii, and thus a modification has been made later on.

In the case of chord sidewall failure (see Fig. 3), the chord sidewall is assumed to be effective along the brace-to-chord sidewall connection

**Fig. 2.** Codified analytical model for brace failure in full-width RHS-to-RHS X and T joints.

length of $h_1/\sin \theta_1$ with a dispersion slope of 2.5 : 1 [8,9]. This assumption results in an effective length of $B_e = h_1/\sin \theta_1 + 5t_0$ in each chord sidewall of a joint under brace axial tension and brace bending. The reduction factor for column buckling (χ_c) can be obtained according to EN 1993-1-1 [39] or an equivalent code, using the relevant buckling curve. Based on the bearing-buckling method [8,9], Table 2 presents the current design rules codified in ISO 14346 [11], CIDECT design guide No. 3 [13] and IIW recommendations [16] for full-width RHS X and T joints using steel grades up to S460, which also impose the limitation on f_y to $0.8f_u$. Note that the design rules for chord sidewall failure in the case of brace in-plane bending are based on a full plastic stress distribution assuming that, for brace angle $\theta_1 = 90^\circ$, the stress within the bearing length of $(h_1 + 5t_0)$ all reaches a stress equal to

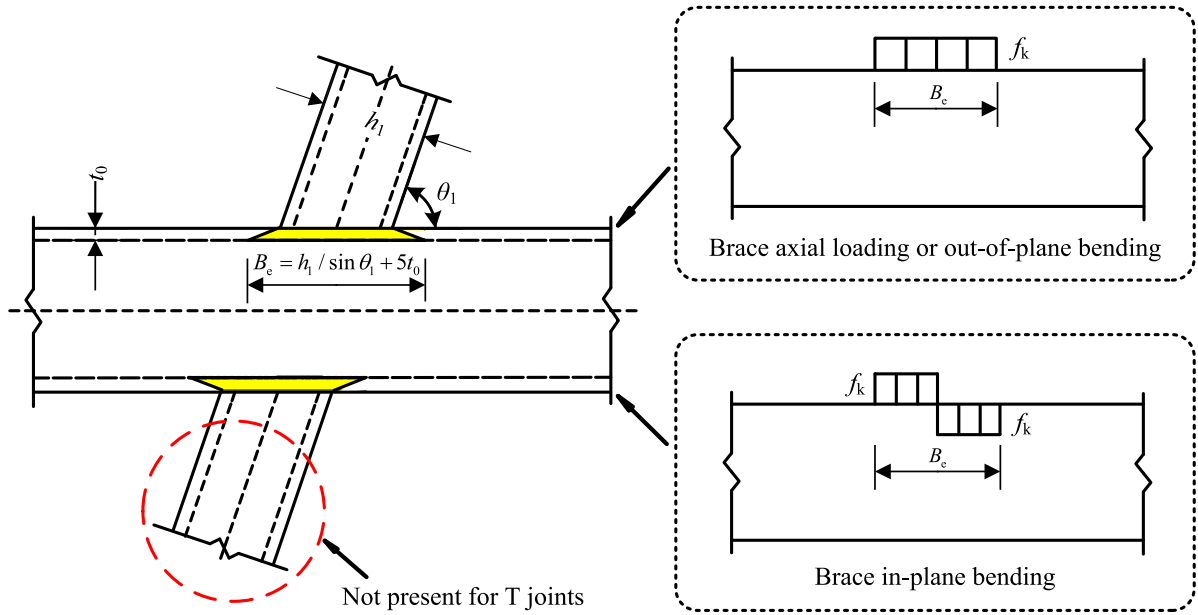


Fig. 3. Codified analytical model for chord sidewall failure in full-width RHS-to-RHS X and T joints.

Table 2

Codified design resistance equations for **chord sidewall failure** in RHS X and T joints [11,13,16].

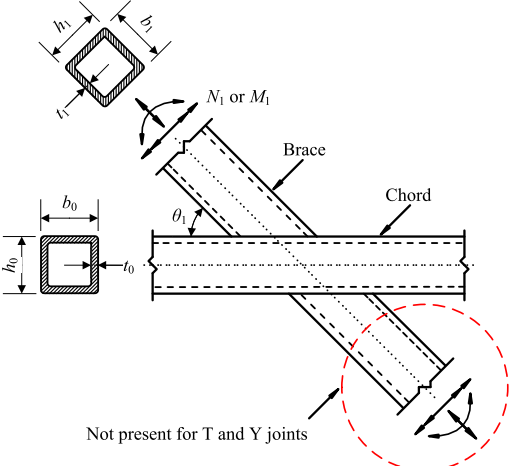
Design resistance	Brace axial loading	
	$N_{1,Rd} = C_{f0} \frac{f_k t_0}{\sin \theta_1} \left(\frac{2h_1}{\sin \theta_1} + 10t_0 \right) Q_f$	Tension: $f_k = f_{y0}$ Compression: $f_k = 0.8\chi_C f_{y0} \sin \theta_1$ for X joints $f_k = \chi_C f_{y0}$ for T joints
	Brace in-plane bending	
	$M_{ip,1,Rd} = 0.5C_{f0} f_k t_0 (h_1 + 5t_0)^2 Q_f$	$f_k = 0.8\chi_C f_{y0}$ for X joints $f_k = f_{y0}$ for T joints
	Brace out-of-plane bending	
	$M_{op,1,Rd} = C_{f0} f_k t_0 (b_0 - t_0)(h_1 + 5t_0) Q_f$	$f_k = 0.8\chi_C f_{y0}$ for X joints $f_k = \chi_C f_{y0}$ for T joints
	Parameters	
	1. Reduction factor for column buckling (χ_C) is determined according to, e.g., EN 1993-1-1 [39] or equivalents using the relevant buckling curve and a normalised slenderness defined by:	
	$\lambda_C = \frac{3.46 \left(\frac{b_0}{t_0} - 2 \right) \sqrt{\frac{1}{\sin \theta_1}}}{\pi \sqrt{\frac{E}{f_{y0}}}}$	
	2. Chord material factor (C_{f0}) is taken as: $C_{f0} = 1.0$ for $f_{y0} \leq 355$ MPa and $C_{f0} = 0.9$ for $355 < f_{y0} \leq 460$ MPa	
	3. Steel yield stress (f_y) for design shall be: $f_{y0} \leq 460$ MPa, $f_{y1} \leq 460$ MPa, $f_{y0} \leq 0.8f_{u0}$, $f_{y1} \leq 0.8f_{u1}$, $f_{y1} \leq f_{y0}$	
	4. Chord stress function (Q_f) is taken as: $Q_f = (1 - n)^{0.1}$ with n in connecting chord face defined by $n = \frac{N_{0,Ed}}{N_{pl0,Rd}} + \frac{M_{0,Ed}}{M_{pl0,Rd}}$ for Class 1 or 2 chord cross-sections under chord compression stress and for chord cross-sections under chord tension stress	
	Validity ranges $b_0/t_0 \leq 40$, $h_0/t_0 \leq 40$, Class 1 or 2 cross-section for the brace and chord under compression stress; $0.5 \leq h_0/b_0 \leq 2.0$; $\theta_1 \geq 30^\circ$	

the local buckling stress (f_k). The buckling reduction factor, which is based on test results, is taken as 1.0 for T joints under brace in-plane bending [7,9]. Additionally, with the exception of this f_y/f_u limit, the design rules in Tables 1–2 are also included in EN 1993-1-8 [10]. The validity range is further extended to steel grades up to S700 in EN 1993-1-12 [40], but with a material factor of 0.8 for steel grades higher than S460 and up to S700.

It should be noted that the codified design rules in Table 1 have a tight limitation on cross-section class and stipulate only Class 1

or 2 cross-sections be used for the brace and chord under compression stresses. However, the cross-section of a number of commercially available RHS tubes, in particular for high-strength steel, falls in the category of Class 3. Such a design provision narrows down the choice of RHS for designers and could necessitate the use of considerably thick-walled RHS, which may cause added expenses and fabrication issues, such as welding. Thus, the need to relax the cross-section limit is apparent. It is worth mentioning that the cross-section class indicates the extent to which the strength and rotation capacity of a cross-section

Table 3Design resistance equations for **chord sidewall failure** in RHS-to-RHS X, T and Y joints under **brace axial compression** [37,38].

Design resistance	Brace axial compression
 <p>Not present for T and Y joints</p>	$N_{Rd,Lan} = C_{f0} f_k t_0 (2h_1 + 10t_0) Q_f \sqrt{\frac{1}{\sin \theta_1}}$
	Parameters
	1. Buckling stress (f_k) is taken as: $f_k = \chi_{0.5} \left(\frac{h_0}{h_1} \right)^{0.15} f_{y0} \text{ but } \leq f_{y0}$
	2. Buckling reduction factor ($\chi_{0.5}$) is determined by: $\chi_{0.5} = 1.12 - 0.012 \frac{h_0}{t_0} \sqrt{\frac{f_{y0}}{355}}$ Alternatively, $\chi_{0.5}$ value may also be derived according to e.g., EN1993-1-1 [39] or equivalents using the buckling curve c and a non-dimensional slenderness: $\lambda_{0.5} = \frac{1.73 \left(\frac{h_0}{t_0} - 2 \right)}{\pi \sqrt{\frac{E}{f_{y0}}}}$
	3. Chord material factor (C_{f0}) is taken as: $C_{f0} = 1.1 - 0.1 f_{y0} / 355 \text{ but } \leq 1.0$
	4. Steel yield stress (f_y) for design shall be: $f_{y0} \leq 960 \text{ MPa}, f_{y1} \leq 960 \text{ MPa}$
	5. Chord stress function (Q_f) is taken as: $Q_f = (1 - n)^{0.1} \text{ with } n \text{ in connecting chord face defined by}$ $n = \frac{N_{0,Ed}}{N_{pl,0,Rd}} + \frac{M_{0,Ed}}{M_{pl,0,Rd}} \text{ for Class 1 and 2 chord cross-sections under chord compression}$ stress and for chord cross-sections under chord tension stress; $M_{el,0,Rd}$ should be used for Class 3 chord cross-sections
Validity ranges	
$b_0/t_0 \leq 40, h_0/t_0 \leq 40; 0.25 \leq h_1/h_0 \leq 2.0; 0.5 \leq h_0/b_0 \leq 2.0; \theta_1 \geq 30^\circ$	

are limited by its local buckling resistance. For example, four classes (Class 1–4), together with three limits on the cross-sectional width-to-thickness ratio for RHS, are stipulated in EN 1993-1-1 [39]. Class 1–2 and Class 3 cross-sections can attain at least the plastic and elastic moment capacity, respectively, while the moment capacity of Class 4 cross-sections is lower than the elastic moment capacity due to elastic local buckling.

2.2. Recent research advances

It is well-known that the codified design resistance equations for chord sidewall failure under brace axial compression (see Table 2) can be considerably conservative, in particular for very slender chord cross-sections, because they are still based on a lower-bound of limited test data in the 1970s and early 1980s [9]. Various alternative strength equations have been proposed, and a detailed summary is available in Refs. [37,38].

The codified resistance equations for chord sidewall failure under brace axial compression have recently been comprehensively evaluated against existing test and numerical results in the literature, and details are available in Wardenier et al. [37] and Lan et al. [38]. The resulting recommended design resistance equations for chord sidewall failure in RHS-to-RHS X, T and Y joints under brace axial compression, as summarised in Table 3, have been adopted by IIW Sub-commission XVE to update ISO 14346 [11] and IIW recommendations [16]. It should be noted that the resistance factor (or partial safety factor), which equals 1.0, has already been included in the design resistance equations in Table 3, which are based on the modified bearing–buckling method and the simplified Lan–Kuhn method [37,38]. When compared with the codified design rules in Table 2, the major updates of the design resistance equations in Table 3 are as follows [38]:

- (1) A large database of existing test and numerical results of mild steel and high-strength steel RHS joints is established, and the validity range of the proposed design rules has been extended to steel grades up to S960. A material factor (i.e. $C_{f0} = 1.1 - 0.1 f_{y0} / 355$) is proposed to consider the material effect for RHS X and T joints under brace axial compression.

- (2) The codified brace angle function is largely simplified by only including an overall angle function of $(1/\sin \theta_1)^{0.5}$ in the final design equation, which is in line with Platt [41] and Davies and Roodbaraky [42].
- (3) The brace-to-chord height ratio (h_1/h_0) is shown to have a significant effect on the chord sidewall resistance, and thus the corresponding effect is considered by including a function of $(h_1/h_0)^{-0.15}$ in the buckling stress equation (f_k).
- (4) The chord sidewall resistance of RHS-to-RHS joints is based on a clamped condition at the top and bottom sides of a chord sidewall with a buckling length of $0.5(h_0 - 2t_0)$, resulting in a higher buckling coefficient ($\chi_{0.5}$), which is in accordance with Yu [21] and Kuhn et al. [35].
- (5) The design resistance equations are valid provided that the chord is sufficiently supported out-of-plane to avoid the skewing failure and out-of-plane instability.

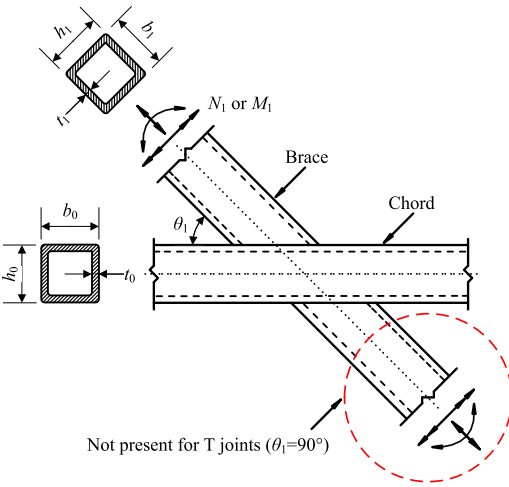
From the re-analyses conducted by Wardenier et al. [37] and Lan et al. [38], it can also be concluded that the proposed basic equations for chord sidewall failure, in principle, can be used for the loading case of brace axial tension. It only has to be checked whether different partial factors need to be applied, depending on ductility of failure modes (ductile or brittle). Furthermore, it has to be examined whether the proposed material factor equation is also applicable for the loading case of brace axial tension. Similarly, the same observations apply to chord sidewall failure in RHS joints under brace bending.

3. Proposed design resistance equations

3.1. Brace failure

Following the review in Section 2, the codified effective width method [8,9] is modified herein, and the resulting design resistance equations proposed for brace failure in RHS X and T joints under brace axial tension are summarised in Table 4. In contrast to the codified brace cross-sectional effective area (i.e. $A_e = (2h_1 + 2b_e - 4t_1)t_1$) in Table 1, the brace cross-sectional effective area (A_e) is suggested

Table 4
Proposed design resistance equations for **brace failure** in RHS X and T joints.

Design resistance	Brace axial tension
	$N_{BF} = C_{f1} f_{y1} [A_1 - 2(b_1 - b_e)t_1]$
	Brace in-plane bending
	$M_{ip,BF} = C_{f1} f_{y1} [W_{pl,1} - (b_1 - b_e)(h_1 - t_1)t_1]$ for Class 1 or 2 cross-sections $M_{ip,BF} = C_{f1} f_{y1} [W_{el,1} - (b_1 - b_e)(h_1 - t_1)t_1]$ for Class 3 cross-sections
	Brace out-of-plane bending
	$M_{op,BF} = C_{f1} f_{y1} [W_{pl,1} - 0.5(b_1 - b_e)^2 t_1]$ for Class 1 or 2 cross-sections $M_{op,BF} = C_{f1} f_{y1} [W_{el,1} - 0.33(b_1 - b_e)^2 t_1]$ for Class 3 cross-sections
Parameters	
1. Brace effective width (b_e) is determined from:	
$b_e = \frac{10}{b_0/t_0} \frac{f_{y0} t_0}{f_{y1} t_1} b_1 \text{ but } \leq b_1$	
2. Brace material factor (C_{f1}) is taken as:	
$C_{f1} = 1.1 - 0.1 f_{y1}/355 \text{ but } \leq 1.0$	
Validity ranges	
Limitations of $f_{y0} \leq 0.8 f_{u0}$ and $f_{y1} \leq 0.8 f_{u1}$ to be checked	

to be modified using $A_e = A_1 - 2(b_1 - b_e)t_1$, where A_1 is the brace cross-sectional gross area. This is because the latter equation (A_e) can give a more-accurate prediction of the brace cross-sectional effective area for both hot-formed and cold-formed hollow sections, and is also more consistent with the current equation format for brace in-plane bending and brace out-of-plane bending, as shown in Table 1. It is noted that the codified A_e function gives an acceptable approximation of the effective area for hot-formed hollow sections, but it can overestimate the effective area for cold-formed hollow sections, having larger corner radii, by up to about 10%. Furthermore, compared with the codified resistance equations (see Table 1), more optimistic brace material factors (C_{f1}) are adopted in line with Refs. [37,38]. The corresponding rounded-off C_{f1} values are 1.00, 0.95, 0.90, 0.85 and 0.80 for steel grades of S355, S460, S700, S900 and S960, respectively.

Table 4 also presents the proposed design resistance equations for brace failure in RHS X and T joints under brace in-plane bending and brace out-of-plane bending, using the modified effective width method. The limitation of cross-section class is modified to include Class 3 (see Section 2.1). Accordingly, elastic member properties, i.e., elastic section modulus (W_{el}), are used for Class 3 brace cross-sections. Furthermore, in contrast to a plastic stress distribution in the effective area of Class 1–2 brace cross-sections with a coefficient of 0.5 ($=2 \times 1/4$), an elastic stress distribution with a coefficient of 0.33 ($=2 \times 1/6$) is adopted in the design resistance equation for Class 3 brace cross-sections under out-of-plane bending. It is noted that compared with the codified design resistance equations (see Table 1), a more optimistic equation of brace material factor (C_{f1}) is used in line with Refs. [37,38].

3.2. Chord sidewall failure

The proposed design resistance equations for chord sidewall failure in RHS X and T joints under brace axial tension, which are based on the modified bearing–buckling method and the Lan–Kuhn method [37,38], are tabulated in Table 5. It is noted that the chord sidewall in a RHS joint under brace axial tension is not vulnerable to local buckling, and therefore the unreduced chord yield stress (f_{y0}) can be used in the determination of chord sidewall resistances. Additionally, the chord material factor equation (C_{f0}) proposed in Refs. [37,38] is adopted herein, and the corresponding rounded-off C_{f0} values are 1.00, 0.95, 0.90, 0.85 and 0.80 for steel grades of S355, S460, S700, S900 and

S960, respectively. Furthermore, as discussed in Section 2.1, it is proposed to relax the cross-section limit to include Class 3. Thus, where applicable, elastic member properties (i.e., W_{el}) shall be used for Class 3 cross-sections, e.g., to determine the chord stress in the chord stress function (Q_f).

The proposed design resistance equations for chord sidewall failure in RHS X and T joints under brace in-plane bending and brace out-of-plane bending, which are based on the modified bearing–buckling method and the Lan–Kuhn method [37,38], are also tabulated in Table 5. Similar to the loading case of brace axial tension, the chord material factor (C_{f0}) proposed in Refs. [37,38] is employed, and elastic member properties are adopted for Class 3 chord cross-sections in determination of the chord stress. It should be noted that the constants of 0.5 ($=2 \times 1/4$) and 0.33 ($=2 \times 1/6$) in the design resistance equations for brace in-plane bending follow from the plastic and elastic stress distributions for the two chord sidewalls, respectively. Furthermore, a function of $(h_1/h_0)^{-0.15}$ is included in the f_k equation in Table 5 for brace out-of-plane bending, similar to the loading case of brace axial compression in Table 3. However, it is noted that for RHS joints under brace in-plane bending, the compression part as shown in Fig. 3 is smaller than h_1 and closer to $0.5h_1$. Therefore, for brace in-plane bending, the function of $(h_1/h_0)^{-0.15}$ has been changed to be $(0.5h_1/h_0)^{-0.15}$ to mirror the actual stress distribution within the bearing length (B_c).

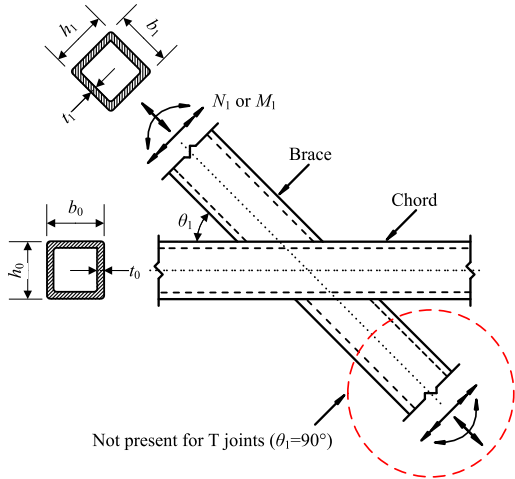
4. Evaluation for full-width RHS joints under brace axial tension

4.1. General

Tables 4–5 summarise the proposed design resistance equations for brace failure and chord sidewall failure in full-width RHS X and T joints under brace axial tension. The adopted material factor (i.e., $C_f = 0.97$ for S460), originally proposed for RHS X and T joints under brace axial compression [37,38], is more optimistic than the currently codified material factor (i.e., $C_f = 0.90$ for S460). A database totalling 43 full-width RHS X joints under brace axial tension (see Table 6), which were tested by Davies et al. [6], Mang et al. [19], Björk [22], Björk and Saastamoinen [23], Tuominen and Björk [24], Feldmann et al. [25] and Becque and Wilkinson [26], was established to assess the proposed design resistance equations. Likewise, a total of seven RHS T joints under brace axial tension were collated from Wardenier and de Koning [4], as shown in Table 7.

Table 5Proposed design resistance equations for **chord sidewall failure** in RHS X and T joints.

Design resistance	Brace axial tension
	$N_{CSF} = C_{f0} f_{y0} t_0 (2h_1 + 10t_0) Q_f \sqrt{\frac{1}{\sin \theta_1}}$
	Brace in-plane bending
	$M_{ip,CSF} = 0.5 C_{f0} f_k t_0 (h_1 + 5t_0)^2 Q_f$ for Class 1 or 2 cross-sections
	$M_{ip,CSF} = 0.33 C_{f0} f_k t_0 (h_1 + 5t_0)^2 Q_f$ for Class 3 cross-sections
	Brace out-of-plane bending
	$M_{op,CSF} = C_{f0} f_k t_0 (h_1 + 5t_0) (b_1 - t_0) Q_f$
	Parameters
	1. Buckling stress (f_k) is taken as:
	$f_k = \chi_{0.5} \left(\frac{h_0}{h_1/2} \right)^{0.15} f_{y0}$ but $\leq f_{y0}$ for brace in-plane bending
	$f_k = \chi_{0.5} \left(\frac{h_0}{h_1} \right)^{0.15} f_{y0}$ but $\leq f_{y0}$ for brace out-of-plane bending
	2. Buckling reduction factor ($\chi_{0.5}$) is determined by:
	$\chi_{0.5} = 1.12 - 0.012 \frac{h_0}{t_0} \sqrt{\frac{f_{y0}}{355}}$
	Alternatively, $\chi_{0.5}$ value may also be derived according to e.g., EN1993-1-1 [39] or equivalents using the buckling curve c and a non-dimensional slenderness:
	$\lambda_{0.5} = \frac{1.73 \left(\frac{h_0}{t_0} - 2 \right)}{\pi \sqrt{\frac{E}{f_{y0}}}}$
	3. Chord material factor (C_{f0}) is taken as:
	$C_{f0} = 1.1 - 0.1 f_{y0}/355$ but ≤ 1.0
	4. Chord stress function (Q_f) is taken as:
	$Q_f = (1 - n)^{0.1}$ with n in connecting chord face defined by
	$n = \frac{N_{0,Ed}}{N_{pl,0,Rd}} + \frac{M_{0,Ed}}{M_{pl,0,Rd}}$ for Class 1 and 2 chord cross-sections under chord compression
	stress and for chord cross-sections under chord tension stress; $M_{el,0,Rd}$ should be used for Class 3 chord cross-sections
	Validity ranges
	Limitations of $f_{y0} \leq 0.8 f_{u0}$ and $f_{y1} \leq 0.8 f_{u1}$ to be checked



For the collated test results as summarised in Tables 6–7, the negative and positive values of the chord stress ratio (n) represent compression and tension chord stresses, respectively. The maximum applied loads in tests (N_{1u}) are used for the joint strengths in all following analyses. This is because the stiffness of full-width RHS X and T joints is high, and thus the 3% b_0 deformation limit [13] is generally not governing in the determination of joint capacity or the difference in joint capacity considering the deformation limit or not is marginal. The applied load at the deformation limit of 3% b_0 and load–deformation curves are also not reported in the earlier studies. Additionally, the failure in tests in Tables 6–7 refers to the failure location or the observed failure mode of the joints, as reported. It is anticipated that fracture can initiate in the brace, chord or weld at the brace–chord intersection in the post-ultimate stage when the joints are under large tension loading, as shown in Fig. 4. However, the design criteria for brace failure or chord sidewall failure may have been reached before the initiation of fracture. In such cases, the predicted failure modes can deviate from the observed final failure modes reported in the literature.

Tables 8–9 show a comparison of the predicted design resistance ($N_{P_{red}}$), which is taken as the lower of the design resistances for brace failure and chord sidewall failure obtained from Tables 4–5 (N_{BF} and N_{CSF}), with the maximum applied load in tests (N_{1u}). It is noted that the actual cross-sectional area and elastic and/or plastic section modulus of the brace and chord were not reported in some studies. For the analyses of these joints, the nominal values in EN 10210 [43] or EN 10219 [44], as relevant, multiplied by the measured-to-nominal wall thickness ratio, were used. In addition, the Lan–Kuhn method with buckling reduction factor ($\chi_{0.5}$), which is linearised against the ratio of chord height to wall thickness (h_0/t_0) as shown in Table 5, was adopted for chord sidewall failure in RHS joints. The N_{1u}/N_y ratio, where $N_y (= A_1 f_{y1})$ is the full yield resistance of the brace cross-section, was

employed to examine whether the maximum applied load has exceeded the full brace yield resistance.

Note that the characteristic (or nominal) resistance for RHS joints, taking account of data scatter and fabrication tolerances, is usually close to 0.9 times the mean of test data. ISO 14346 [11] and IIW recommendations [16] adopt, for ductile failures, a reduction factor of 0.9 (or a partial factor of 1.1) to convert the characteristic resistance to the design resistance, and thus the ratio of the mean of the test data to the design resistance is about 1.2 (=1.10/0.9). For non-ductile failures, a reduction factor of 0.8 (or a partial factor of 1.25) is used to convert the characteristic resistance to the design resistance, which coincides with a factor of 1.4 (=1.25/0.9) between the mean of the test data and the design resistance. The factor of 1.4, which was also adopted for developing codified design rules in the 1970s and 1980s, is roughly equal to the ultimate-to-yield stress ratio for S355. This factor is thus employed to qualitatively evaluate the safety margins of the proposed design resistance equations in the following sections, and associated reliability analyses are conducted in Section 7.

4.2. Assessment for full-width RHS X joints

4.2.1. Test results of Davies et al. [6] and Mang et al. [19]

Davies et al. [6] tested two hot-formed full-width RHS X joints using mild steel of S235. These two specimens failed, after chord sidewall failure and brace yielding, finally by fracture through the welds, which was affected by weld slag inclusions. Both specimens had, at the brace–chord intersection, fillet welds on the chord face with a throat thickness of $a = t_1$, and groove welds at the chord side, with a brace end preparation of 20–25° (see Fig. 5(a)). As shown in Table 8, the N_{1u}/N_{Pred} ratios are 1.31 for specimen B-1 with chord sidewall failure governing, and 1.20 for specimen B-4 controlled by brace failure. The corresponding N_{1u}/N_{y1} ratios are 0.99 and 1.20.

Table 6

Collated test results totalling 43 RHS X joints under brace axial tension.

Reference	Specimen	b_0 (mm)	h_0 (mm)	t_0 (mm)	b_1 (mm)	h_1 (mm)	t_1 (mm)	f_{y0} (MPa)	f_{y1} (MPa)	n	N_{lu} (kN)	Observed failure
Davies et al. [6]	B-1	181.0	181.0	9.00	179.5	179.4	6.00	259	336	0	1375	weld
	B-4	181.0	180.7	13.40	180.0	179.5	6.00	254	336	0	1664	weld
Mang et al. [19]	1e	100.0	100.0	4.30	100.0	100.0	4.30	367	367	0	438	chord weld toe
	2e	100.0	100.0	7.80	100.0	100.0	4.10	326	367	0	573	brace weld toe
	8c	100.0	100.0	4.00	100.0	100.0	4.00	367	367	-0.70	375	chord weld toe
	8d	100.0	100.0	6.25	100.0	100.0	4.00	243	367	-0.98	440	brace weld toe
	8e	100.0	100.0	6.25	100.0	100.0	4.00	243	367	0	489	brace weld toe
Björk [22]	X3A	100.2	100.3	7.82	100.0	100.0	7.82	472	472	0.60	1142	chord sidewall
	X3B	100.2	100.3	7.82	100.0	100.0	7.82	472	472	0.60	1368	brace weld toe
	X4	100.2	100.3	7.82	100.2	100.3	7.82	472	472	0.60	1295	chord sidewall
	X6	99.8	99.8	7.66	99.8	99.8	7.66	425	425	0.60	1306	chord sidewall
	X8	99.8	99.9	7.65	99.8	99.9	7.65	482	482	0.60	1388	chord sidewall
	X13	99.8	99.9	10.06	99.8	99.9	10.06	443	443	0.60	1602	brace
	X18	99.8	99.9	9.93	99.8	99.9	9.93	468	468	0.60	1750	brace
	X19	99.8	99.9	9.97	99.8	99.9	9.97	505	505	0.60	1844	brace
	X22	99.9	99.8	9.51	99.9	99.8	9.51	424	424	0.60	1720	chord sidewall
	X24	99.8	100.1	9.85	99.8	100.1	9.85	499	499	0.60	2025	brace
	X26	100.2	100.3	7.81	100.2	100.3	7.81	503	503	0.60	1516	chord sidewall
	X28	100.5	100.3	5.83	100.5	100.3	5.83	511	511	0.60	1140	chord sidewall
Björk and Saastamoinen [23]	X1	119.7	120.2	5.93	120.0	119.8	5.98	516	516	0	1262	brace weld toe
	X2	120.1	119.9	5.90	120.0	119.7	5.95	516	516	0	1272	chord fracture
	X4	120.1	120.4	9.85	120.0	120.2	4.08	483	519	0	1069	brace
	X6	200.7	200.7	6.00	200.9	100.3	4.00	473	506	0	980	brace weld toe
	X7	200.7	200.7	6.00	201.5	200.4	4.95	473	479	0	1511	brace weld toe
	X8	200.5	200.7	6.03	199.9	99.9	6.00	473	466	0	1118	chord fracture
	X9	120.1	120.4	9.85	120.1	120.1	9.88	483	483	0	2075	brace weld toe
	X12	119.9	119.9	4.00	120.2	120.2	3.94	451	451	0	820	brace weld toe
	X12C	119.7	120.6	4.04	119.7	120.3	4.01	451	451	0	776	brace weld toe
	X1B	120.1	119.9	5.90	120.1	119.8	5.98	516	516	0	1335	chord fracture
	X2B	120.0	119.8	5.90	119.8	119.8	5.96	516	516	0	1321	chord fracture
	X12B	119.9	119.9	4.00	120.2	120.2	3.94	519	519	0	828	chord fracture
Tuominen and Björk [24]	CX1RT_420S	100.0	100.0	5.91	100.0	100.0	5.91	529	529	0	1031	brace weld toe
	CX1RT_420R	100.0	100.0	6.04	100.0	100.0	6.04	488	488	0	908	chord seam weld
	CX1RT_420Rb	100.0	100.0	6.04	100.0	100.0	6.04	488	488	0	978	brace weld toe
	CX1-40_420S	100.0	100.0	5.91	100.0	100.0	5.91	547	547	0	1129	brace weld toe
	CX1-40_420R	100.0	100.0	6.04	100.0	100.0	6.04	488	488	0	1053	brace weld toe
	CX1RT_460V	100.0	100.0	6.28	100.0	100.0	6.28	536	536	0	1174	weld fracture
Feldmann et al. [25]	CX1-40_460V	100.0	100.0	6.28	100.0	100.0	6.28	536	536	0	1246	weld fracture
	S500-RX1	100.0	100.0	4.12	100.0	100.0	4.12	522	522	0	718	brace weld toe
	S700-RX1	100.0	100.0	4.82	100.0	100.0	4.82	725	725	0	1154	brace weld toe
Becque and Wilkinson [26]	S960-RX1	100.0	100.0	3.98	100.0	100.0	3.98	996	996	0	816	chord weld toe
	X4 (45°)	198.7	100.5	3.93	198.7	100.6	3.93	438	438	0	588	chord fracture
	X6 (90°)	199.5	199.5	5.83	198.7	100.6	3.93	449	438	0	659	brace weld toe

Note: Specimen X4 [26] had a brace angle $\theta_1 = 45^\circ$, and $\theta_1 = 90^\circ$ for other specimens.**Table 7**

Collated test results totalling 7 RHS T joints under brace axial tension.

Reference	Specimen	b_0 (mm)	h_0 (mm)	t_0 (mm)	b_1 (mm)	h_1 (mm)	t_1 (mm)	f_{y0} (MPa)	f_{y1} (MPa)	n	N_{lu} (kN)	Observed failure
Wardenier and de Koning [4]	1	99.5	99.5	3.72	99.5	99.5	3.72	317	317	-0.94	301	chord local buckling
	1'	99.5	99.5	3.72	99.5	99.5	3.72	317	317	-0.92	296	chord local buckling
	4	100.4	100.4	6.30	99.5	99.5	3.72	305	317	-1.01	496	weld
	4'	100.4	100.4	6.30	99.5	99.5	3.72	305	317	-0.98	484	weld
	7	100.1	100.1	4.05	100.1	100.1	4.05	345	345	-0.89	332	chord local buckling
	10	99.9	99.9	6.04	100.1	101.1	4.05	365	345	-0.87	470	brace, weld
	10'	99.9	99.9	6.04	100.1	101.1	4.05	365	345	-1.03	572	brace

Another series of hot-formed mild steel full-width RHS X joints was collated from Mang et al. [19]. All five specimens failed by weld-related fractures. However, specimen 2e is predicted to be governed by brace failure, and the chord sidewall failure criterion governs for the other four specimens. All the X joint specimens had fillet welds on the chord face with a small throat thickness of $a = t_1$, considering the steel grade S355 of the brace, and groove welds at the chord side, where the brace ends were bevelled at 45° , as illustrated in Fig. 5(b). All specimens finally failed by fractures in the weld or at the weld toe of the brace or chord, which demonstrates the importance of the welding detail. Excluding specimen 2e, which just reached the brace yield resistance (i.e. $N_{lu}/N_{y1} = 1.00$), and specimen 8d, having a high chord stress ratio

$n = -0.98$, for which the Q_f function is considerably conservative, the N_{lu}/N_{Pred} ratio of the other three specimens varies from 1.15 to 1.23.

4.2.2. Test results of Björk [22] and Björk and Saastamoinen [23]

Björk [22] tested cold-formed full-width RHS X joints using S355 at varying temperatures (-40°C and $+20^\circ\text{C}$) and a tension preload of 60% of the chord yield load ($A_0 f_{y0}$) was applied to the chord. All specimens had, at the brace–chord intersection, fillet welds on the chord face with $a = 1.1t_1$, and groove welds at the chord side. It is noted that specimens X3A, X3B and X4 had nearly identical geometric dimensions and material properties but deviating resistances. This is caused by the

Table 8

Evaluation of proposed design resistance equations against test results of 43 RHS X joints under brace axial tension.

Specimen	f_{y0} (MPa)	Chord section	f_{y1} (MPa)	Brace section	n	h_0/t_0	N_{lu} (kN)	N_{lu}/N_{y1}	N_{BF} (kN)	N_{CSF} (kN)	N_{Pred} (kN)	N_{lu}/N_{Pred}	Predicted failure
B-1	259	Class 1-2	336	Class 1-2	0	20.1	1375	0.99	1078	1047	1047	1.31	CSF
B-4	254	Class 1-2	336	Class 1-2	0	13.5	1664	1.20	1384	1675	1384	1.20	BF
1e	367	Class 1-2	367	Class 1-2	0	23.3	438	0.73	418	382	382	1.15	CSF
2e	326	Class 1-2	367	Class 1-2	0	12.8	573	1.00	569	706	569	1.01	BF
8c	367	Class 1-2	367	Class 1-2	-0.70	25.0	375	0.67	380	311	311	1.20	CSF
8d	243	Class 1-2	367	Class 1-2	-0.98	16.0	440	0.79	452	270	270	1.63	CSF
8e	243	Class 1-2	367	Class 1-2	0	16.0	489	0.88	452	399	399	1.23	CSF
X3A	472	Class 1-2	472	Class 1-2	0.60	12.8	1142	0.91	1057	908	908	1.26	CSF
X3B	472	Class 1-2	472	Class 1-2	0.60	12.8	1368	1.09	1057	908	908	1.51	CSF
X4	472	Class 1-2	472	Class 1-2	0.60	12.8	1295	1.03	1057	908	908	1.43	CSF
X6	425	Class 1-2	425	Class 1-2	0.60	13.0	1306	1.18	937	804	804	1.62	CSF
X8	482	Class 1-2	482	Class 1-2	0.60	13.0	1388	1.11	1043	896	896	1.55	CSF
X13	443	Class 1-2	443	Class 1-2	0.60	9.9	1602	1.10	1417	1191	1191	1.34	CSF
X18	468	Class 1-2	468	Class 1-2	0.60	10.1	1750	1.16	1462	1228	1228	1.43	CSF
X19	505	Class 1-2	505	Class 1-2	0.60	10.0	1844	1.12	1571	1318	1318	1.40	CSF
X22	424	Class 1-2	424	Class 1-2	0.60	10.5	1720	1.31	1251	1063	1063	1.62	CSF
X24	499	Class 1-2	499	Class 1-2	0.60	10.1	2025	1.26	1525	1285	1285	1.58	CSF
X26	503	Class 1-2	503	Class 1-2	0.60	12.8	1516	1.14	1114	957	957	1.58	CSF
X28	511	Class 1-2	511	Class 1-2	0.60	17.2	1140	1.06	785	673	673	1.69	CSF
X1	516	Class 1-2	516	Class 1-2	0	20.2	1262	0.93	936	873	873	1.45	CSF
X2	516	Class 1-2	516	Class 1-2	0	20.4	1272	0.94	929	867	867	1.47	CSF
X4	483	Class 1-2	519	Class 3	0	12.2	1069	1.12	914	1554	914	1.17	BF
X6	473	Class 4	506	Class 4	0	33.5	980	0.85	657	715	657	1.49	BF
X7	473	Class 4	479	Class 4	0	33.5	1511	0.83	1165	1264	1165	1.30	BF
X8	473	Class 4	466	Class 4	0	33.3	1118	0.71	766	717	717	1.56	CSF
X9	483	Class 1-2	483	Class 1-2	0	12.2	2075	1.07	1666	1553	1553	1.34	CSF
X12	451	Class 1-2	451	Class 3	0	30.0	820	1.02	507	492	492	1.67	CSF
X12C	451	Class 1-2	451	Class 1-2	0	29.6	776	0.95	518	498	498	1.56	CSF
X1B	516	Class 1-2	516	Class 1-2	0	20.4	1335	0.98	932	868	868	1.54	CSF
X2B	516	Class 1-2	516	Class 1-2	0	20.3	1321	0.98	931	868	868	1.52	CSF
X12B	519	Class 3	519	Class 3	0	30.0	828	0.89	572	555	555	1.49	CSF
CX1RT_420S	529	Class 1-2	529	Class 1-2	0	16.9	1031	0.92	827	770	770	1.34	CSF
CX1RT_420R	488	Class 1-2	488	Class 1-2	0	16.6	908	0.86	797	739	739	1.23	CSF
CX1RT_420Rb	488	Class 1-2	488	Class 1-2	0	16.6	978	0.92	797	739	739	1.32	CSF
CX1-40_420S	547	Class 1-2	547	Class 1-2	0	16.9	1129	0.97	851	792	792	1.42	CSF
CX1-40_420R	488	Class 1-2	488	Class 1-2	0	16.6	1053	0.99	797	739	739	1.43	CSF
CX1RT_460V	536	Class 1-2	536	Class 1-2	0	15.9	1174	0.97	912	840	840	1.40	CSF
CX1-40_460V	536	Class 1-2	536	Class 1-2	0	15.9	1246	1.03	912	840	840	1.48	CSF
S500-RX1	522	Class 1-2	522	Class 1-2	0	24.3	718	0.90	522	494	494	1.45	CSF
S700-RX1	725	Class 1-2	725	Class 1-2	0	20.7	1154	0.90	828	777	777	1.49	CSF
S960-RX1	996	Class 4	996	Class 4	0	25.1	816	0.55	819	779	779	1.05	CSF
X4 (45°)	438	Class 4	438	Class 4	0	50.6	588	0.60	426	480	426	1.38	BF
X6 (90°)	449	Class 4	438	Class 4	0	34.2	659	0.67	591	661	591	1.11	BF

Note: BF refers to brace failure, and CSF represents chord sidewall failure.

Table 9

Evaluation of proposed design resistance equations against test results of 7 RHS T joints under brace axial tension.

Specimen	f_{y0} (MPa)	Chord section	f_{y1} (MPa)	Brace section	n	h_0/t_0	N_{lu} (kN)	N_{lu}/N_{y1}	N_{BF} (kN)	N_{CSF} (kN)	N_{Pred} (kN)	N_{lu}/N_{Pred}	Predicted failure
1	317	Class 1-2	317	Class 1-2	-0.94	26.7	301	0.67	301	210	210	1.43	CSF
1'	317	Class 1-2	317	Class 1-2	-0.92	26.7	296	0.66	301	215	215	1.37	CSF
4	305	Class 1-2	317	Class 1-2	-1.01	15.9	496	1.11	448	—	—	—	CMF
4'	305	Class 1-2	317	Class 1-2	-0.98	15.9	484	1.08	448	335	335	1.45	CSF
7	345	Class 1-2	345	Class 1-2	-0.89	24.7	332	0.64	354	269	269	1.23	CSF
10	365	Class 1-2	345	Class 1-2	-0.87	16.5	470	0.90	508	—	—	—	CMF
10'	365	Class 1-2	345	Class 1-2	-1.03	16.5	572	1.10	508	—	—	—	CMF

Note: CSF represents chord sidewall failure and CMF denotes chord member failure.

varying geometries of the groove welds connecting the sidewalls of the chord, as depicted in Fig. 6. The inadequate groove weld configuration in specimen X3A, resulting in a more-pronounced stress concentration at the weld and a smaller effective throat, reduced the joint strength by 20% and lowered the corresponding joint deformation capacity when compared with specimen X3B. All test specimens, except for specimen X3A, reached the full brace yield resistance (i.e. $N_{lu}/N_{y1} > 1.0$), exhibiting sufficient plastic deformation capacity, and corresponding N_{lu}/N_{Pred} ratios vary from 1.34 to 1.69. Additionally, the effect of varying temperatures (-40 °C and $+20$ °C) was found to be negligible [22].

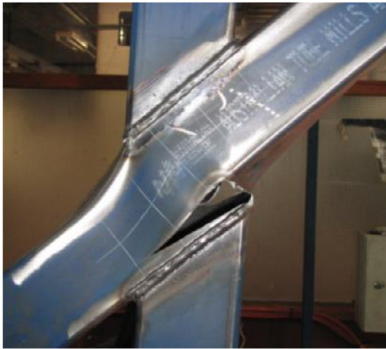
Björk and Saastamoinen [23] also studied cold-formed full-width RHS X joints using double-grade S420/S355. These test specimens were welded, at the brace–chord intersection, using fillet welds on the chord face with a minimum throat thickness of $a = 1.1t_1$, which is the required weld size for S355, and groove welds at the chord side, as depicted in Fig. 6(b). It was found that using a larger weld throat thickness only led to up to 6% higher joint strength, when compared with $a = 1.1t_1$ [23]. Table 8 shows that three specimens with brace failure governing have N_{lu}/N_{Pred} ratios varying from 1.17 to 1.49, and chord sidewall failure controls for the other nine specimens with N_{lu}/N_{Pred} ratios ranging from 1.34 to 1.67.



(a) Brace fracture in specimen CX1-40_420R [24]



(b) Weld fracture in specimen CX1RT_460V [24]



(c) Chord fracture in specimen X4 (45°) [26]

Fig. 4. Fracture failure in the post-ultimate stage of test specimens under brace axial tension.

4.2.3. Test results of Tuominen and Björk [24] and Feldmann et al. [25]

Tuominen and Björk [24] experimentally investigated cold-formed full-width RHS X joints using S420 and S460. All specimens had, at the brace–chord intersection, fillet welds on the chord face with a throat thickness of $a = 1.1t_1$, and groove welds at the chord side. Excluding specimen CX1RT_420R failing in the chord seam weld, all tests showed, after reaching the chord sidewall failure criterion, failures in the weld and/or at the weld toe in the brace or chord, and corresponding N_{lu}/N_{Pred} ratios range from 1.32 to 1.48.

Tuominen and Björk also tested cold-formed full-width RHS X joints using S500, S700 and S960, results of which have been compiled in the RUOSTE report by Feldmann et al. [25]. The three specimens were welded using fillet welds on the chord face with $a = 6.4$ mm ($1.55t_1$) for S500, 7.1 mm ($1.47t_1$) for S700 and 4.58 mm ($1.15t_1$) for S960, and groove welds at the chord side. The weld throat thickness for the S500 and S700 specimens seems to be sufficient while that for the S960 specimen is small. The three specimens showed failures at the brace

weld toe for S500 and S700, and fracture at the chord weld toe for S960.

The N_{lu}/N_{Pred} ratios of specimens S500-RX1 and S700-RX1 are 1.45 and 1.49, respectively, indicating sufficient joint strength for less-ductile failure modes; however, that of specimen S960-RX1 equals 1.05, which is low for less-ductile failures. This may be caused by the more pronounced material softening for higher steel grades and/or the small weld size for the S960 specimen. It is noted that the heat input, which was used for welding S960 specimens in the RUOSTE project, ranged from 0.59 to 1.02 kJ/mm. The material softening in the coupon extracted from the brace–chord junction of specimen S960-RX1 (with brace and chord wall thickness of 3.98 mm) was around 20%, which can contribute to the lower joint strength. It is also noted that the material factors recommended in Ref. [25] are 1.0, 0.9 and 0.8 for S500, S700 and S960, respectively, and these agree reasonably well with those proposed in Refs. [37,38], which are 0.96, 0.90 and 0.83 for S500, S700 and S960, as used in Tables 4–5.

4.2.4. Test results of Becque and Wilkinson [26]

Becque and Wilkinson [26] conducted tests on two cold-formed full-width RHS X joints using C450 steel. It was observed that specimen X4 with $\theta_1 = 45^\circ$ ultimately failed by a less-ductile chord fracture, which was classified as punching shear in the reference, and the predicted failure mode is brace failure with a N_{lu}/N_{Pred} ratio of 1.38. Specimen X6 finally failed at the brace weld toe, and the predicted failure mode is brace failure with $N_{lu}/N_{Pred} = 1.11$.

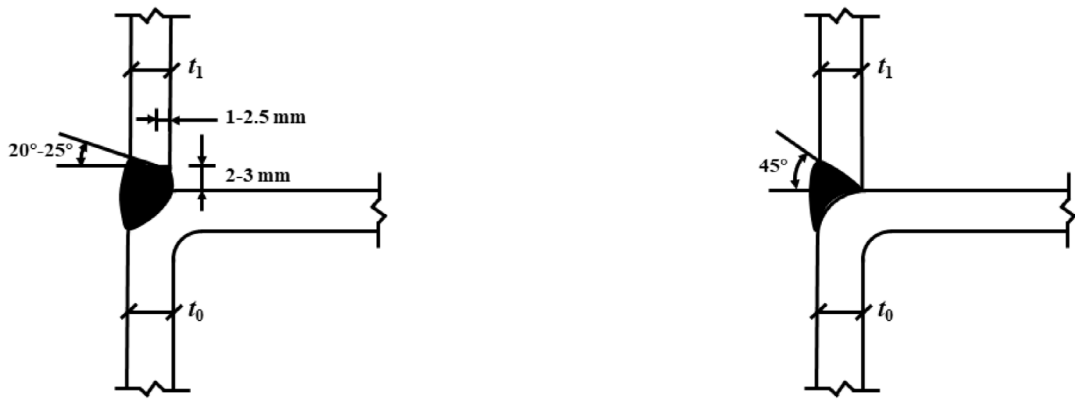
In order to examine the effect of applying the limitations of $f_{y0} \leq 0.8f_{u0}$ and $f_{y1} \leq 0.8f_{u1}$, the test results reported by Feldmann et al. [25] and Becque and Wilkinson [26] were used for re-analyses, as summarised in Table 10. It is shown that applying such limitations increases the N_{lu}/N_{Pred} ratio from 1.45 to 1.52 for specimen S500-RX1 and from 1.49 to 1.66 for specimen S700-RX1, which is not necessary. However, the N_{lu}/N_{Pred} ratio of specimen S960-RX1 increases from 1.05 to 1.18, which is still not sufficient, and thus this ultra-high steel grade requires further research. Likewise, the N_{lu}/N_{Pred} ratio marginally increases from 1.38 to 1.47 for specimen X4, and from 1.11 to 1.18 for specimen X6. Therefore, applying such limitations for steel grades up to S700 is not adequately justified, and more investigations are needed for higher steel grades.

4.3. Assessment for full-width RHS T joints

It is common that chord lengths of RHS T joints in test specimens under brace axial loading are designed to be short to avoid bending failure of the chord before joint failure. However, this could lead to a combination of chord bending moments and large chord shear stresses at the brace–chord intersection, and the supports at the two chord ends may affect the stress distribution in the joint region.

The test results of S235 hot-formed RHS T joints [4], using fillet welds on the chord face with $a = t_1$, were used to evaluate the design resistance equations for RHS T joints under brace axial tension (see Tables 4–5). The tests were carried out to check the effect of different welding procedures (i.e., electrode or MIG). That is why some data have the same specimen number (e.g., 1 for rutile electrode and 1' for MIG CO₂).

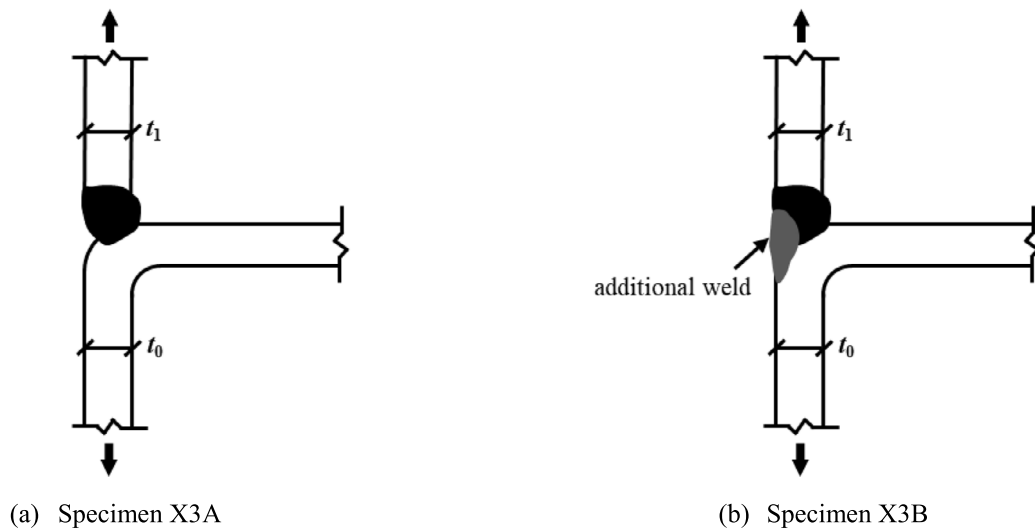
Table 9 shows that specimens 4, 4' and 10' with low h_0/t_0 ratios reached the full brace yield resistance (i.e., $N_{lu}/N_{y1} \geq 1.0$). The chord compression stresses in specimens 4 and 10' with $n < -1.0$ were large. Specimen 10 had considerably large chord bending and shear stresses, and was predicted to fail by a combination of chord bending and shear. Thus, specimens 4, 10 and 10' with chord member failure were excluded. The N_{lu}/N_{Pred} ratio of specimens 1, 1', 4' and 7, without reported weld defects, ranges from 1.23 to 1.45. It should be noted that the hot-formed RHS T joints under brace axial tension tested by Mang et al. [7] all failed in the chord member due to large chord bending moments, and thus these test data were not considered.



(a) Dutch tests (Wardenier et al. [4] and Davies et al. [6])

(b) German tests (Mang et al. [19])

Fig. 5. Weld details adopted in reported tests.



(a) Specimen X3A

(b) Specimen X3B

Fig. 6. Two nearly identical RHS X joint specimens but with varying weld profiles. (Björk [22])

Table 10

Evaluation of the effect of applying limitations of $f_{y0} \leq 0.8f_{u0}$ and $f_{y1} \leq 0.8f_{u1}$ for RHS X joints under brace axial tension.

Specimen	f_{y0} (MPa)	Chord section	f_{y1} (MPa)	Brace section	n	h_0/t_0	N_{lu} (kN)	N_{lu}/N_{y1}	N_{BF} (kN)	N_{CSF} (kN)	N_{Pred} (kN)	N_{lu}/N_{Pred}	Predicted failure
S500-RX1	522	Class 1–2	522	Class 1–2	0	24.3	718	0.90	500	473	473	1.52	CSF
S700-RX1	725	Class 1–2	725	Class 1–2	0	20.7	1154	0.90	742	697	697	1.66	CSF
S960-RX1	996	Class 4	996	Class 4	0	25.1	816	0.55	729	694	694	1.18	CSF
X4 (45°)	438	Class 4	438	Class 4	0	50.6	588	0.60	401	451	401	1.47	BF
X6 (90°)	449	Class 4	438	Class 4	0	34.2	659	0.67	556	636	556	1.18	BF

Note: BF refers to brace failure, and CSF represents chord sidewall failure.

5. Evaluation for RHS joints under brace bending

5.1. RHS X joints under brace in-plane bending

The hot-formed full-width RHS X joints under brace in-plane bending in Table 11 are collated from Mang et al. [19] and Yu [21]. In the tests by Mang et al. [19], the chord was axially loaded to apply brace in-plane bending moments, which induced chord stresses. Specimen 9a failed by weld cracking and local buckling of the brace, and weld failure was observed in specimen 9b. In the numerical study by Yu [21], in-plane bending was applied at the brace ends and a steel grade of S690 was selected for the brace to avoid brace failure, thereby resulting in chord sidewall failure for all the specimens.

Table 12 shows a comparison of the predicted design resistance ($M_{ip,Pred}$), which is taken as the lower of the design resistances for

brace failure and chord sidewall failure derived from Tables 4–5 ($M_{ip,BF}$ and $M_{ip,CSF}$), with the maximum applied bending moments in tests and numerical simulations ($M_{ip,lu}$). The Lan–Kuhn method with the buckling reduction factor ($\chi_{0.5}$) linearised against the h_0/t_0 ratio (see Table 5) was used for chord sidewall failure. The $M_{ip,lu}/M_{ip,pl}$ ratio, where $M_{ip,pl} (= W_{ip,pl} f_{y1})$ is the plastic moment resistance of the brace cross-section, was used to examine whether the maximum applied bending moment has exceeded the full brace plastic moment resistance in tests and numerical simulations.

It should be noted that if one of the cross-sections of the brace and the chord is classified as Class 3 (also Class 4), the design resistance equations for the brace and the chord for Class 3 (instead of Class 1–2) cross-sections should be employed in order to be consistent with the actual load transfer. For example, for Class 3 cross-sections, if one uses a plastic stress distribution within the bearing length (B_e) for

Table 11
Collated test and numerical results totalling 10 RHS X joints under brace in-plane bending.

Reference	Specimen	b_0 (mm)	h_0 (mm)	t_0 (mm)	b_1 (mm)	h_1 (mm)	t_1 (mm)	f_{y0} (MPa)	f_{y1} (MPa)	n	$M_{ip,lu}$ (kNm)	Observed failure
Mang et al. [19]	9a	100	100	6.30	100	100	4.00	279	367	−0.13	19.0	brace, weld
	9b	100	100	4.00	100	100	4.00	367	367	−0.13	16.5	weld
Yu [21]	x10ie05	150	150	10.00	150	75	10.00	355	690	0	37.1	chord sidewall
	x10ie	150	150	10.00	150	150	10.00	355	690	0	89.7	chord sidewall
	x10ie2	150	150	10.00	150	300	10.00	355	690	0	259.7	chord sidewall
	x11i	150	150	6.25	150	150	6.25	355	690	0	50.0	chord sidewall
	x11ie2	150	150	6.25	150	300	6.25	355	690	0	128.7	chord sidewall
	x12ie05	150	150	4.29	150	75	4.29	355	690	0	12.2	chord sidewall
	x12i	150	150	4.29	150	150	4.29	355	690	0	28.6	chord sidewall
	x12ie2	150	150	4.29	150	300	4.29	355	690	0	76.5	chord sidewall

Note: All specimens had $\theta_1 = 90^\circ$.

Table 12
Evaluation of proposed design resistance equations, using f_k for chord sidewall failure, against results of 10 RHS X joints under brace in-plane bending.

Specimen	f_{y0} (MPa)	Chord section	f_{y1} (MPa)	Brace section	n	h_0/t_0	$M_{ip,lu}$ (kNm)	$M_{ip,lu}/M_{ip,pl}$	$M_{ip,BF}$ (kNm)	$M_{ip,CSF}$ (kNm)	$M_{ip,Pred}$ (kNm)	$M_{ip,lu}/M_{ip,Pred}$	Predicted failure
9a	279	Class 1–2	367	Class 1–2	−0.13	15.9	19.0	0.95	16.4	15.0	15.0	1.27	CSF
9b	367	Class 1–2	367	Class 1–2	−0.13	25.0	16.5	0.83	11.5	9.4	9.4	1.76	CSF
x10ie05	355	Class 1–2	690	Class 1–2	0	15.0	37.1	0.50	27.6	27.7	27.6	1.35	BF
x10ie	355	Class 1–2	690	Class 1–2	0	15.0	89.7	0.45	92.5	71.0	71.0	1.26	CSF
x10ie2	355	Class 1–2	690	Class 4	0	15.0	259.7	0.46	226.2	134.9	134.9	1.93	CSF
x11i	355	Class 1–2	690	Class 1–2	0	24.0	50.0	0.38	52.9	33.6	33.6	1.49	CSF
x11ie2	355	Class 1–2	690	Class 4	0	24.0	128.7	0.35	132.4	66.8	66.8	1.93	CSF
x12ie05	355	Class 3	690	Class 4	0	35.0	12.2	0.33	5.6	4.0	4.0	3.03	CSF
x12i	355	Class 3	690	Class 4	0	35.0	28.6	0.31	21.9	11.5	11.5	2.49	CSF
x12ie2	355	Class 3	690	Class 4	0	35.0	76.5	0.30	87.6	36.4	36.4	2.10	CSF

Note: BF refers to brace failure, and CSF represents chord sidewall failure.

chord sidewall failure, but elastic section properties for the brace, this contradicts the actual load transfer and stress flow from the brace to the chord. Additionally, Class 4 cross-sections have lower member capacities than those of Class 3 cross-sections, and the $M_{ip,lu}/M_{ip,Pred}$ ratios will be higher if effective (instead of elastic) cross-section properties are adopted. Applying the design resistance equations of the brace and the chord for Class 3 cross-sections, to joints having Class 4 cross-sections, results in lower $M_{ip,lu}/M_{ip,Pred}$ ratios, and is therefore on the conservative side for the evaluation. More detailed discussions can be found in Wardenier et al. [45].

As shown in Table 12, the $M_{ip,lu}/M_{ip,pl}$ ratios of all the examined specimens are lower than 1.0, indicating that the brace plastic moment resistances have not been reached. It is noted that the predicted failure mode for specimen x10ie05 is brace failure with corresponding $M_{ip,lu}/M_{ip,Pred}$ ratio of 1.35. However, the predicted design resistance for brace failure ($M_{ip,BF} = 27.6$ kNm) is nearly equal to that for chord sidewall failure ($M_{ip,CSF} = 27.7$ kNm), indicating that brace failure and chord sidewall failure are predicted to occur almost simultaneously. All other specimens are predicted to be governed by chord sidewall failure and the corresponding $M_{ip,lu}/M_{ip,Pred}$ ratios vary from 1.26 to 3.03.

Considering that the predicted design resistances are considerably conservative for some specimens failing by chord sidewall failure, the design resistance equations in Table 5, but using $f_k = f_{y0}$, are also evaluated as summarised in Table 13. It is shown that the modified design resistance equations reduce the conservatism with corresponding $M_{ip,lu}/M_{ip,Pred}$ ratios ranging from 1.26 to 2.61. Therefore, the modified design resistance equations in Table 5, using $f_k = f_{y0}$, can be used for mild steel, but the applicability for higher steel grades needs to be further verified. Thus, the original design resistance equations in Table 5, using f_k , are recommended for high-strength steel, until more test and numerical evidence is available.

5.2. RHS T joints under brace in-plane bending

The experimental results of full-width RHS T joints under brace in-plane bending in Table 14 are collated from Mang et al. [7] for

hot-formed RHS T joints and from Kanatani et al. [17] and Tabuchi et al. [18] for cold-formed RHS T joints. Mang et al. [7] conducted a comprehensive test study on moment-loaded RHS T joints using S235 and S355. However, it is not always possible to re-analyse these tests because some data could not be found in the original reports, and therefore the collated results are mainly based on the reported data by Mang et al. [7] but partly extracted from Mang et al. [19] and de Koning and Wardenier [46]. Although, in principle, only test data with measured geometric dimensions are compiled in this study, the results collated from Kanatani et al. [17] and Tabuchi et al. [18], with only nominal geometric dimensions, are an exception, and have been included because of their detailed investigations on weld sizes and slender sections.

It is noted that specimen M-S20-22/1.0–0.67/6 had a small throat thickness for the fillet welds on the chord face (i.e., $a = 0.98t_1$), which was $1.17 \leq a \leq 1.52$ for other specimens tested by Kanatani et al. [17]. Further, Fig. 7 shows that an inadequate weld profile in specimen M-S20-22/1.0–0.67/6 resulted in weld fracture and, more importantly, a less-ductile joint behaviour, when compared with comparable specimen M-S20-22/1.0–0.67/6E with larger weld size of $a = 1.17t_1$. Such weld defects also occurred in specimens N-S20-17/1.0–0.5/9 and K-S20-17/1.0–0.5/9 [17,18]. Fig. 8 illustrates that specimen N-S20-17/1.0–0.5/9E, with a brace end preparation, exhibits higher joint strength and deformation capacity than those of specimen N-S20-17/1.0–0.5/9, without such a preparation.

Table 15 summarises a comparison of the predicted design resistance ($M_{ip,Pred}$), which is taken as the lower of $M_{ip,BF}$ and $M_{ip,CSF}$ derived from Tables 4–5, with the maximum applied bending moments in tests ($M_{ip,lu}$). Similar to the case of RHS X joints under brace in-plane bending, if one of the cross-sections of the brace and the chord is classified as Class 3 (also Class 4), the design resistance equations for the brace and the chord for Class 3 (instead of Class 1–2) cross-sections are adopted, in order to be consistent with the actual load transfer. The Lan–Kuhn method with the buckling reduction factor ($\chi_{0.5}$) linearised against the h_0/t_0 ratio (see Table 5) was used for chord sidewall failure. Additionally, the $M_{ip,lu}/M_{ip,pl}$ ratio was used to examine whether the

Table 13Evaluation of proposed design resistance equations, using $f_k = f_{y0}$ for chord sidewall failure, against results of 10 RHS X joints under brace in-plane bending.

Specimen	f_{y0} (MPa)	Chord section	f_{y1} (MPa)	Brace section	n	h_0/t_0	$M_{ip,lu}$ (kNm)	$M_{ip,lu}/$ $M_{ip,pl}$	$M_{ip,BF}$ (kNm)	$M_{ip,CSF}$ (kNm)	$M_{ip,Pred}$ (kNm)	$M_{ip,lu}/$ $M_{ip,Pred}$	Predicted failure
9a	279	Class 1–2	367	Class 1–2	−0.13	15.9	19.0	0.95	16.4	15.0	15.0	1.27	CSF
9b	367	Class 1–2	367	Class 1–2	−0.13	25.0	16.5	0.83	11.5	10.4	10.4	1.59	CSF
x10ie05	355	Class 1–2	690	Class 1–2	0	15.0	37.1	0.50	27.6	27.7	27.6	1.35	BF
x10ie	355	Class 1–2	690	Class 1–2	0	15.0	89.7	0.45	92.5	71.0	71.0	1.26	CSF
x10ie2	355	Class 1–2	690	Class 4	0	15.0	259.7	0.46	226.2	143.5	143.5	1.81	CSF
x11i	355	Class 1–2	690	Class 1–2	0	24.0	50.0	0.38	52.9	36.4	36.4	1.37	CSF
x11ie2	355	Class 1–2	690	Class 4	0	24.0	128.7	0.35	132.4	80.3	80.3	1.60	CSF
x12ie05	355	Class 3	690	Class 4	0	35.0	12.2	0.33	5.6	4.7	4.7	2.61	CSF
x12i	355	Class 3	690	Class 4	0	35.0	28.6	0.31	21.9	14.8	14.8	1.94	CSF
x12ie2	355	Class 3	690	Class 4	0	35.0	76.5	0.30	87.6	51.9	51.9	1.47	CSF

Note: BF refers to brace failure, and CSF represents chord sidewall failure.

Table 14

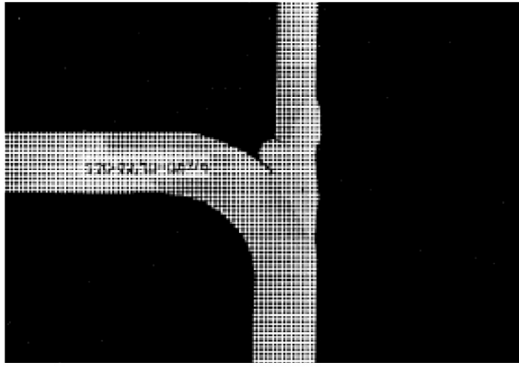
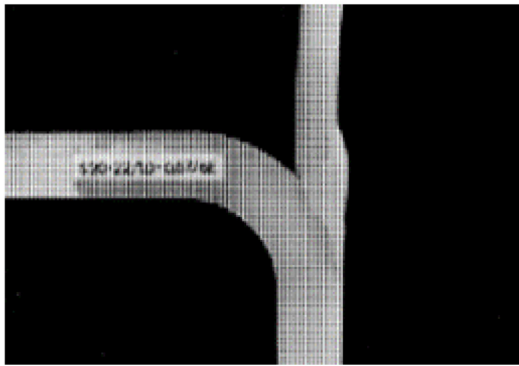
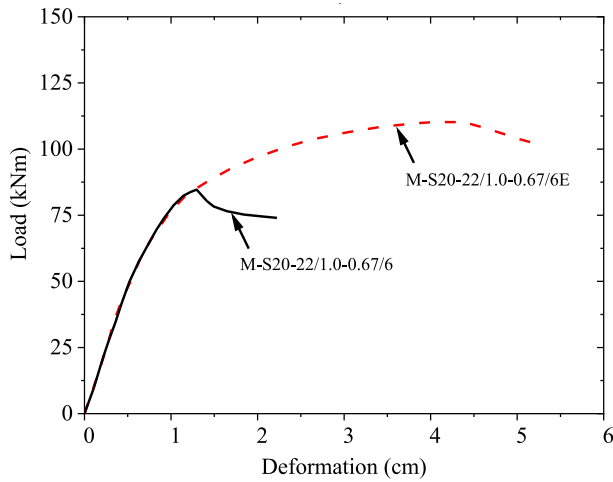
Collated test results totalling 20 RHS T joints under brace in-plane bending.

Reference	Specimen	b_0 (mm)	h_0 (mm)	t_0 (mm)	b_1 (mm)	h_1 (mm)	t_1 (mm)	f_{y0} (MPa)	f_{y1} (MPa)	n	$M_{ip,lu}$ (kNm)	Observed failure
Mang et al. [7]	1a	120	120	3.50	120	120	3.50	332	332	−0.28	17.1	chord sidewall
	1b	120	120	3.55	120	120	3.60	332	332	−0.36	16.5	chord sidewall
	1c	120	120	3.50	120	120	3.50	332	332	−0.55	16.3	chord sidewall
	1d	120	120	3.55	120	120	3.55	332	332	−0.63	14.3	chord sidewall
	1e	100	100	2.86	100	100	2.84	314	314	−0.25	8.6	chord sidewall
	1f	100	100	3.00	100	100	3.00	314	314	−0.79	9.0	chord sidewall
	1g	100	100	3.10	100	100	2.95	314	314	−1.00	7.9	chord sidewall
Kanatani et al. [17]	C-S20-33/1.0-1.0/9	200	200	6	200	200	6	383	383	−0.46	89.6	chord flange
	M-S20-22/1.0-0.67/6	200	200	9	200	200	6	383	383	−0.31	83.0	weld
	M-S20-22/1.0-0.67/6E	200	200	9	200	200	6	355	392	−0.44	108.6	weld
	M-S20-22/1.0-0.67/9E	200	200	9	200	200	6	355	392	−0.45	112.6	weld
	M-S20-22/1.0-0.67/9	200	200	9	200	200	6	355	392	−0.47	116.3	weld
	N-S20-17/1.0-0.5/6E	200	200	12	200	200	6	378	392	−0.40	129.3	brace
	N-S20-17/1.0-0.5/9E	200	200	12	200	200	6	378	392	−0.40	129.4	brace
	N-S20-17/1.0-0.5/9	200	200	12	200	200	6	378	392	−0.35	113.3	weld
	L-S30-50/1.0-1.0/9	300	300	6	300	300	6	457	457	−0.25	129.5	chord sidewall
Tabuchi et al. [18]	F-S20-33/1.0-1.0/9	200	200	6	200	200	6	390	390	−0.46	91.4	chord sidewall
	K-S20-17/1.0-0.5/6E	200	200	12	200	200	6	385	400	−0.40	131.9	brace
	K-S20-17/1.0-0.5/9	200	200	12	200	200	6	385	400	−0.35	115.6	weld
	K-S20-17/1.0-0.5/9E	200	200	12	200	200	6	385	400	−0.40	132.0	brace

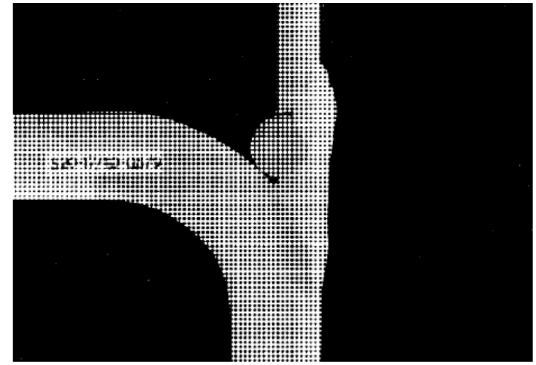
Table 15Evaluation of proposed design resistance equations, using f_k for chord sidewall failure, against results of 20 RHS T joints under brace in-plane bending.

Specimen	f_{y0} (MPa)	Chord section	f_{y1} (MPa)	Brace section	n	h_0/t_0	$M_{ip,lu}$ (kNm)	$M_{ip,lu}/$ $M_{ip,pl}$	$M_{ip,BF}$ (kNm)	$M_{ip,CSF}$ (kNm)	$M_{ip,Pred}$ (kNm)	$M_{ip,lu}/$ $M_{ip,Pred}$	Predicted failure
1a	332	Class 1–2	332	Class 1–2	−0.28	34.3	17.1	0.74	11.5	7.7	7.7	2.23	CSF
1b	332	Class 1–2	332	Class 1–2	−0.36	33.8	16.5	0.70	11.8	7.8	7.8	2.12	CSF
1c	332	Class 1–2	332	Class 1–2	−0.55	34.3	16.3	0.71	11.5	7.3	7.3	2.23	CSF
1d	332	Class 1–2	332	Class 1–2	−0.63	33.8	14.3	0.61	11.7	7.4	7.4	1.94	CSF
1e	314	Class 1–2	314	Class 1–2	−0.25	35.0	8.6	0.82	4.3	4.1	4.1	2.08	CSF
1f	314	Class 1–2	314	Class 1–2	−0.79	33.3	9.0	0.81	4.7	4.0	4.0	2.27	CSF
1g	314	Class 1–2	314	Class 1–2	−1.00	32.3	7.9	0.72	4.9	–	–	–	CMF
C-S20-33/1.0-1.0/9	383	Class 3	383	Class 3	−0.46	33.3	89.6	0.71	45.6	29.3	29.3	3.06	CSF
M-S20-22/1.0-0.67/6	383	Class 1–2	383	Class 3	−0.31	22.2	83.0	0.66	78.8	61.0	61.0	1.36	CSF
M-S20-22/1.0-0.67/6E	355	Class 1–2	392	Class 3	−0.44	22.2	108.6	0.84	74.7	56.6	56.6	1.92	CSF
M-S20-22/1.0-0.67/9E	355	Class 1–2	392	Class 3	−0.45	22.2	112.6	0.87	74.7	56.4	56.4	2.00	CSF
M-S20-22/1.0-0.67/9	355	Class 1–2	392	Class 3	−0.47	22.2	116.3	0.90	74.7	56.2	56.2	2.07	CSF
N-S20-17/1.0-0.5/6E	378	Class 1–2	392	Class 3	−0.40	16.7	129.3	1.00	109.8	95.6	95.6	1.35	CSF
N-S20-17/1.0-0.5/9E	378	Class 1–2	392	Class 3	−0.40	16.7	129.4	1.00	109.8	95.6	95.6	1.35	CSF
N-S20-17/1.0-0.5/9	378	Class 1–2	392	Class 3	−0.35	16.7	113.3	0.88	109.8	96.4	96.4	1.18	CSF
L-S30-50/1.0-1.0/9	457	Class 4	457	Class 4	−0.25	50.0	129.5	0.86	106.8	45.3	45.3	2.86	CSF
F-S20-33/1.0-1.0/9	390	Class 3	390	Class 3	−0.46	33.3	91.4	0.71	46.4	29.6	29.6	3.09	CSF
K-S20-17/1.0-0.5/6E	385	Class 1–2	400	Class 3	−0.40	16.7	131.9	1.00	111.8	97.2	97.2	1.36	CSF
K-S20-17/1.0-0.5/9	385	Class 1–2	400	Class 3	−0.35	16.7	115.6	0.88	111.8	97.9	97.9	1.18	CSF
K-S20-17/1.0-0.5/9E	385	Class 1–2	400	Class 3	−0.40	16.7	132.0	1.00	111.8	97.2	97.2	1.36	CSF

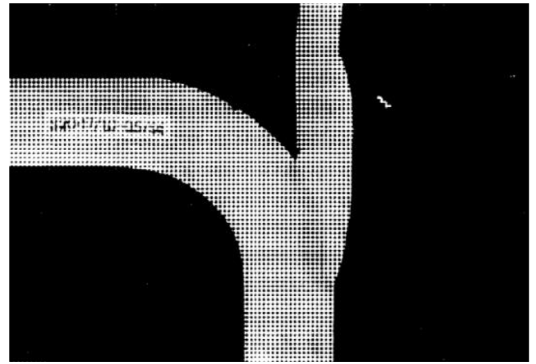
Note: CMF indicates chord member failure, and CSF represents chord sidewall failure.

(a) Specimen M-S20-22/1.0-0.67/6 with measured $a = 5.9$ mm(b) Specimen M-S20-22/1.0-0.67/6E with measured $a = 7.0$ mm

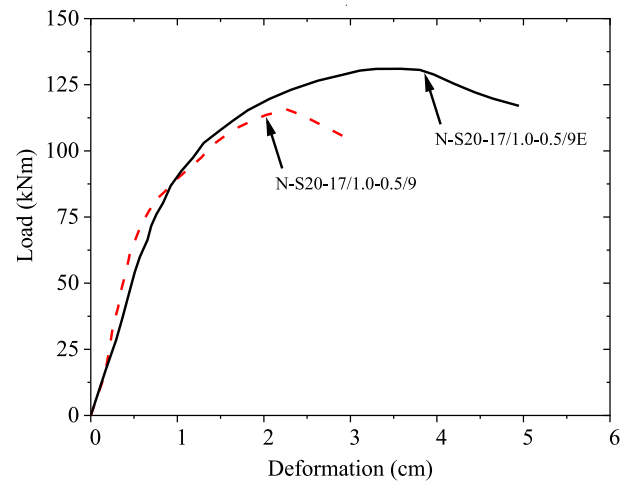
(c) Overall load-deformation curves for M test series



(a) Specimen N-S20-17/1.0-0.5/9 without brace end preparation



(b) Specimen N-S20-17/1.0-0.5/9E with brace end preparation



(c) Overall load-deformation curves for N test series

Fig. 7. Influence of weld size on RHS T joints under brace in-plane bending [7].

Fig. 8. Influence of brace end preparation on RHS T joints under brace in-plane bending [17].

maximum applied moment has exceeded the full brace plastic moment resistance in tests.

As shown in Table 15, four specimens (i.e., N-S20-17/1.0-0.5/6E, N-S20-17/1.0-0.5/9E, K-S20-17/1.0-0.5/6E and K-S20-17/1.0-0.5/9E) have just reached the brace plastic moment resistances with $M_{ip,lu}/M_{ip,pl} = 1.0$, and the other 16 specimens have $M_{ip,lu}/M_{ip,pl} < 1.0$. The chord stress ratio (n) of specimen 1g is -1.0 , and thus the predicted failure mode is chord member failure. All the other specimens are predicted to be governed by chord sidewall failure and the corresponding $M_{ip,lu}/M_{ip,Pred}$ ratios range from 1.18 to 3.09. The predicted

design resistances are shown to be considerably conservative for specimens C-S20-33/1.0-1.0/9 and F-S20-33/1.0-1.0/9 with corresponding $M_{ip,lu}/M_{ip,Pred}$ ratios of 3.06 and 3.09. Likewise, the $M_{ip,lu}/M_{ip,Pred}$ ratio is as high as 2.86 for specimen L-S30-50/1.0-1.0/9, having Class 4 cross-sections with $h_0/t_0 = h_1/t_1 = 50$, which is included because this is the only test having high brace and chord cross-section slenderness. The $M_{ip,lu}/M_{ip,Pred}$ ratio of specimens N-S20-17/1.0-0.5/9 and K-S20-17/1.0-0.5/9, having questionable weld details, is as low as 1.18. All other tests had cross-section slenderness satisfying Class 3 for steel grades of S235 and S355.

Table 16Evaluation of proposed design resistance equations, using $f_k = f_{y0}$ for chord sidewall failure, against results of 20 RHS T joints under brace in-plane bending.

Specimen	f_{y0} (MPa)	Chord section	f_{y1} (MPa)	Brace section	n	h_0/t_0	$M_{ip,lu}$ (kNm)	$M_{ip,lu}/M_{ip,pl}$	$M_{ip,BF}$ (kNm)	$M_{ip,CSF}$ (kNm)	$M_{ip,Pred}$ (kNm)	$M_{ip,lu}/M_{ip,Pred}$	Predicted failure
1a	332	Class 1–2	332	Class 1–2	–0.28	34.3	17.1	0.74	11.5	10.6	10.6	1.61	CSF
1b	332	Class 1–2	332	Class 1–2	–0.36	33.8	16.5	0.70	11.8	10.7	10.7	1.55	CSF
1c	332	Class 1–2	332	Class 1–2	–0.55	34.3	16.3	0.71	11.5	10.1	10.1	1.61	CSF
1d	332	Class 1–2	332	Class 1–2	–0.63	33.8	14.3	0.61	11.7	10.1	10.1	1.41	CSF
1e	314	Class 1–2	314	Class 1–2	–0.25	35.0	8.6	0.82	4.3	5.7	4.3	1.98	BF
1f	314	Class 1–2	314	Class 1–2	–0.79	33.3	9.0	0.81	4.7	5.3	4.7	1.90	BF
1g	314	Class 1–2	314	Class 1–2	–1.00	32.3	7.9	0.72	4.9	–	–	–	CMF
C-S20-33/1.0-1.0/9	383	Class 3	383	Class 3	–0.46	33.3	89.6	0.71	45.6	37.4	37.4	2.39	CSF
M-S20-22/1.0-0.67/6	383	Class 1–2	383	Class 3	–0.31	22.2	83.0	0.66	78.8	65.3	65.3	1.27	CSF
M-S20-22/1.0-0.67/6E	355	Class 1–2	392	Class 3	–0.44	22.2	108.6	0.84	74.7	59.7	59.7	1.82	CSF
M-S20-22/1.0-0.67/9E	355	Class 1–2	392	Class 3	–0.45	22.2	112.6	0.87	74.7	59.6	59.6	1.89	CSF
M-S20-22/1.0-0.67/9	355	Class 1–2	392	Class 3	–0.47	22.2	116.3	0.90	74.7	59.4	59.4	1.96	CSF
N-S20-17/1.0-0.5/6E	378	Class 1–2	392	Class 3	–0.40	16.7	129.3	1.00	109.8	95.6	95.6	1.35	CSF
N-S20-17/1.0-0.5/9E	378	Class 1–2	392	Class 3	–0.40	16.7	129.4	1.00	109.8	95.6	95.6	1.35	CSF
N-S20-17/1.0-0.5/9	378	Class 1–2	392	Class 3	–0.35	16.7	113.3	0.88	109.8	96.4	96.4	1.18	CSF
L-S30-50/1.0-1.0/9	457	Class 4	457	Class 4	–0.25	50.0	129.5	0.86	106.8	93.0	93.0	1.39	CSF
F-S20-33/1.0-1.0/9	390	Class 3	390	Class 3	–0.46	33.3	91.4	0.71	46.4	38.0	38.0	2.40	CSF
K-S20-17/1.0-0.5/6E	385	Class 1–2	400	Class 3	–0.40	16.7	131.9	1.00	111.8	97.2	97.2	1.36	CSF
K-S20-17/1.0-0.5/9	385	Class 1–2	400	Class 3	–0.35	16.7	115.6	0.88	111.8	97.9	97.9	1.18	CSF
K-S20-17/1.0-0.5/9E	385	Class 1–2	400	Class 3	–0.40	16.7	132.0	1.00	111.8	97.2	97.2	1.36	CSF

Note: BF refers to brace failure, CMF indicates chord member failure, and CSF represents chord sidewall failure.

The predicted design resistances are considerably conservative for some specimens failing by chord sidewall failure, and that is why the current design codes and guides adopt $f_k = f_{y0}$ for mild steel RHS T joints loaded by brace in-plane-bending moments. Thus, the design resistance equations in Table 5, but using $f_k = f_{y0}$, are also evaluated as shown in Table 16. It is demonstrated that the modified design resistance equations reduce the conservatism with corresponding $M_{ip,lu}/M_{ip,Pred}$ ratios ranging from 1.18 to 2.40. For example, the $M_{ip,lu}/M_{ip,Pred}$ ratios of specimens C-S20-33/1.0–1.0/9 and F-S20-33/1.0–1.0/9 reduce from around 3.1 to roughly 2.4. Excluding specimens M-S20-22/1.0–0.67/6, N-S20-17/1.0–0.5/9 and K-S20-17/1.0–0.5/9, the $M_{ip,lu}/M_{ip,Pred}$ ratios of other specimens range from 1.35 to 2.40. Therefore, the modified design resistance equations, using $f_k = f_{y0}$, can be used for mild steel, but the applicability for higher steel grades needs to be further verified. Thus, the original design resistance equations in Table 5, using f_k , are suggested for high-strength steel, until more test and numerical evidence is available.

Mang et al. [19] and Yu [21] also compared the behaviour and capacity of RHS X joints with those of RHS T joints. It was found that full-width RHS X and T joints under brace in-plane bending exhibit similar structural behaviour and their strengths agree with each other well. Thus, for the loading case of brace in-plane bending, design resistance equations for brace failure and chord sidewall failure in RHS X joints can also be adopted for the two failure modes in RHS T joints.

5.3. RHS X and T joints under brace out-of-plane bending

The numerical data of hot-formed full-width RHS X joints under brace out-of-plane bending in Table 17 are collated from Yu [21]. In the numerical analyses by Yu [21], equilibrating out-of-plane bending moments were applied at the brace ends and a steel grade of S690 was selected for the brace to avoid brace failure. Table 18 summarises the comparison of the predicted design resistance ($M_{op,Pred}$), which is taken as the lower of design resistances for brace failure and chord sidewall failure determined from Tables 4–5 ($M_{op,BF}$ and $M_{op,CSF}$), with the maximum applied bending moments in numerical simulations ($M_{op,lu}$).

It should be noted that if one of the cross-sections of the brace and the chord is classified as Class 3 (also Class 4), the design resistance equations for a Class 3 brace are used in order to be consistent with the actual load transfer. The Lan–Kuhn method with the buckling reduction factor ($\chi_{0.5}$) linearised against the h_0/t_0 ratio in Table 5 was used for chord sidewall failure. In addition, the $M_{op,lu}/M_{op,pl}$ ratio, where

$M_{op,pl}$ ($= W_{op,pl} f_{y1}$) is the plastic moment resistance of the brace cross-section, was used to examine whether the maximum applied bending moment has exceeded the full brace plastic moment resistance in finite element simulations. Table 18 shows that the $M_{op,lu}/M_{op,pl}$ ratios of all the examined specimens are not higher than 0.64, indicating that the maximum applied bending moment is lower than the brace plastic moment resistance. The predicted failure mode for all the specimens is chord sidewall failure and corresponding $M_{op,lu}/M_{op,Pred}$ ratios range from 1.24 to 1.40 with a mean of 1.33.

Yu [21] also numerically examined the behaviour of RHS T joints under brace out-of-plane bending. However, the analysed joints generally failed by distortion of the chord cross-section, and the resistance and stiffness of these joints largely depend on the unstiffened chord length. Therefore, the design codes and guides [10,11,13,16] prescribe to prevent chord distortion failure. It is noted that full-width RHS X and T joints under brace out-of-plane bending (with X joints having equilibrating brace bending moments), exhibit similar structural behaviour. Such joints can be directly related to a joint under brace axial compression on one side, and to a joint under brace axial tension on the other side, where the minimum resistance governs [37,38]. Thus, if chord distortion, which can easily occur due to fabrication imperfections, is prevented, the same design resistance equations can be adopted for full-width RHS X and T joints under brace out-of-plane bending as for brace axial loading.

6. Performance of full-width RHS X and T joints

6.1. Effect of weld details

The studies summarised in Sections 4–5 show that, especially in the early tests in the 1970s and 1980s, lower joint strengths and deformation capacity in some RHS joints occurred due to weld-related failures, producing a large test scatter. In contrast, RHS joints where no weld-related failures were observed show that the ratio of the test or numerical strength to the predicted design resistance, in general, is close to or exceeds the factor of 1.4. Thus, weld details are demonstrated to be significant for the performance of full-width RHS joints under brace axial tension and brace bending, in which fracture failures can occur in the weld and/or in the heat-affected zone.

A representative example for the influence of weld details is the two nearly identical full-width RHS X joints but with different weld profiles at the chord side (see Fig. 6), which exhibit considerably different joint behaviour. In specimen X3A, the weld at the chord side has a severe

Table 17

Collated numerical results totalling 8 RHS X joints under brace out-of-plane bending.

Reference	Specimen	b_0 (mm)	h_0 (mm)	t_0 (mm)	b_1 (mm)	h_1 (mm)	t_1 (mm)	f_{y0} (MPa)	f_{y1} (MPa)	n	$M_{op,lu}$ (kNm)	Observed failure
Yu [21]	x10oe05	150	150	10.00	150	75	10.00	355	690	0	80.4	CSF
	x10oe	150	150	10.00	150	150	10.00	355	690	0	119.4	CSF
	x10oe2	150	150	10.00	150	300	10.00	355	690	0	192.5	CSF
	x11o	150	150	6.25	150	150	6.25	355	690	0	59.4	CSF
	x11oe2	150	150	6.25	150	300	6.25	355	690	0	108.6	CSF
	x12oe05	150	150	4.29	150	75	4.29	355	690	0	23.0	CSF
	x12o	150	150	4.29	150	150	4.29	355	690	0	37.2	CSF
	x12oe2	150	150	4.29	150	300	4.29	355	690	0	62.7	CSF

Note: CSF represents chord sidewall failure.

Table 18

Evaluation of proposed design resistance equations against results of 8 RHS X joints under brace out-of-plane bending.

Specimen	f_{y0} (MPa)	Chord section	f_{y1} (MPa)	Brace section	n	h_0/t_0	$M_{op,lu}$ (kNm)	$M_{op,lu}/$ $M_{op,pl}$	$M_{op,BF}$ (kNm)	$M_{op,CSF}$ (kNm)	$M_{op,Pred}$ (kNm)	$M_{op,lu}/$ $M_{op,Pred}$	Predicted failure
x10oe05	355	Class 1–2	690	Class 1–2	0	15.0	80.4	0.64	82.8	62.1	62.1	1.29	CSF
x10oe	355	Class 1–2	690	Class 1–2	0	15.0	119.4	0.61	148.4	93.4	93.4	1.28	CSF
x10oe2	355	Class 1–2	690	Class 4	0	15.0	192.5	0.56	250.4	147.4	147.4	1.31	CSF
x11o	355	Class 1–2	690	Class 1–2	0	24.0	59.4	0.45	91.9	48.1	48.1	1.24	CSF
x11oe2	355	Class 1–2	690	Class 4	0	24.0	108.6	0.48	164.1	79.2	79.2	1.37	CSF
x12oe05	355	Class 3	690	Class 4	0	35.0	23.0	0.38	29.9	16.6	16.6	1.38	CSF
x12o	355	Class 3	690	Class 4	0	35.0	37.2	0.40	57.4	26.6	26.6	1.40	CSF
x12oe2	355	Class 3	690	Class 4	0	35.0	62.7	0.40	115.3	45.0	45.0	1.39	CSF

Note: CSF represents chord sidewall failure.

notch, resulting in a loading eccentricity and more significant stress concentration at the chord weld toe, along with a smaller effective throat. On the other hand, the weld at the chord side in specimen X3B is relatively smooth and has a larger effective throat. Consequently, in specimen X3A failure occurred at the weld toe with the chord, but failure at the weld toe with the brace was observed in specimen X3B. The maximum applied load of specimen X3B was, as mentioned before, 20% larger than that of specimen X3A and, more importantly, the corresponding deformation capacity was three times that of specimen X3A.

It is noted that varying weld details have been adopted in the reported experimental studies. Fig. 5(a) shows that the Dutch S235 specimens tested by Wardenier et al. [4] and Davies et al. [6] had fillet welds on the chord face with $a = t_1$ and groove welds at the chord side, filled flush, with a brace end preparation of 20–25°, which is close to the 30° bevel used in the Australian tests by Becque and Wilkinson [26]. The German tests by Mang et al. [19] with S235 steel chords and S355 steel braces also had fillet welds on the chord face with $a = t_1$ which is small for S355 and groove welds at the chord side, filled flush, with a brace end preparation of 45°, as shown in Fig. 5(b).

The Finnish specimens using steel grades not greater than S460 (see Fig. 6), tested by Björk [22], Björk and Saastamoinen [23] and Tuominen and Björk [24], had fillet welds on the chord face with $a = 1.1t_1$ and groove welds at the chord side with, where required, a brace end preparation of 45°. For the Finnish specimens in Feldmann et al. [25], the S500 and S700 specimens had fillet welds on the chord face with a roughly equal to $1.5t_1$ and groove welds at the chord side; however, the S960 specimens, which also adopted groove welds at the chord side, had a too small throat thickness for this steel grade with $a = 1.15t_1$, and the joint strength was low. This shows that sufficiently large weld sizes are vital for ensuring adequate joint performance, which is also confirmed by a comparison of specimens M-S20-22/1.0–0.67/6 and M-S20-22/1.0–0.67/6E as shown in Fig. 7. The brace end preparation, where necessary, is also found to be important (see Fig. 8), as discussed in Section 5.2.

The reported tests demonstrate that the scatter in weld-related fractures caused by weld defects or geometrical imperfections can be large. Thus, it is crucial that these defects and imperfections should be avoided, and the required weld size, brace end preparation and welding quality should conform to the relevant welding code. Welders should

be qualified and certified to do these structural welds. For example, AWS D1.1 [47] requires, for side-matched prequalified PJP groove welds at the chord side of full-width RHS X joints, a root opening of 2 mm and the weld to be filled flush with the side of the brace. Furthermore, joint preparation for corner transitions shall provide a smooth transition from one detail to another, and welding shall be carried out continuously around corners, with corners fully built up and all weld starts and stops within flat faces (see Figure 10.6 in AWS D1.1 [47]). For side-matched prequalified CJP groove welds, brace end preparation is also required, with a minimum root opening of 2 mm and the weld filled flush with the side of the brace (see Figure 10.7 and Table 10.7 in AWS D1.1 [47]).

6.2. Effect of geometrical parameters

For an evaluation of the effect of brace angle, there are limited test data of full-width RHS X joints under brace axial tension or brace bending. In the experimental programme carried out by Becque and Wilkinson [26], only specimen X4 (45°) in Table 8 had a smaller brace angle of $\theta_1 = 45^\circ$, and the corresponding N_{lu}/N_{Pred} ratio is 1.38. Therefore, in line with the findings reported by Platt [41] and Davies and Roodbaraky [42], the brace angle effect in full-width RHS X joints under brace axial tension is quantified by the function $(1/\sin \theta_1)^{0.5}$ as shown in Table 5, which is the same as that for brace axial compression [38]. For non-90° RHS X joints under brace in-plane bending and brace out-of-plane bending, the beneficial brace angle effect can be conservatively neglected, and the joint resistances are taken as those of RHS counterparts with $\theta_1 = 90^\circ$, in accordance with current design codes and guides [10,11,13].

The influence of the h_1/h_0 ratio on chord sidewall strength has been demonstrated to be significant [35,37,38]. For brace in-plane bending, the effect of the h_1/h_0 ratio can be quantified by a function of $[h_0/(h_1/2)]^{0.15}$ for high-strength steel joints (see Table 5), and $f_k = f_{y0}$ can be used for mild steel joints to reduce the conservatism of the resistance predictions, as discussed in Sections 5.1–5.2. For brace out-of-plane bending, the effects can be considered by incorporating the function $(h_0/h_1)^{0.15}$ into the equation for the buckling stress (f_k), in line with Refs. [37,38].

The effect of the h_0/t_0 ratio on chord sidewall strength was also evaluated, against the test results reported by Kanatani et al. [17]

Table 19Evaluation of the effect of h_0/t_0 ratio on chord sidewall strengths of RHS T joints under brace in-plane bending.

Specimen	f_{y0} (MPa)	f_{y1} (MPa)	n	h_0/t_0	$M_{ip,lu}$ (kNm)	$M_{ip,lu}/M_{ip,pl}$	$M_{ip,BF}$ (kNm)	$M_{ip,CSF}$ (kNm)	$M_{ip,Pred}$ (kNm)	$M_{ip,lu}/M_{ip,Pred}$	Predicted failure
N-S20-17/1.0-0.5/6E	378	392	-0.40	16.7	129.3	1.00	109.8	95.6	95.6	1.35	CSF
N-S20-17/1.0-0.5/9E	378	392	-0.40	16.7	129.4	1.00	109.8	95.6	95.6	1.35	CSF
K-S20-17/1.0-0.5/6E	385	400	-0.40	16.7	131.9	1.00	111.8	97.2	97.2	1.36	CSF
K-S20-17/1.0-0.5/9E	385	400	-0.40	16.7	132.0	1.00	111.8	97.2	97.2	1.36	CSF
M-S20-22/1.0-0.67/6	355	392	-0.44	22.2	108.6	0.84	74.7	59.7	59.7	1.82	CSF
M-S20-22/1.0-0.67/9	355	392	-0.45	22.2	112.6	0.87	74.7	59.6	59.6	1.89	CSF
M-S20-22/1.0-0.67/9	355	392	-0.47	22.2	116.3	0.90	74.7	59.4	59.4	1.96	CSF
C-S20-33/1.0-1.0/9	383	383	-0.46	33.3	89.6	0.71	45.6	37.4	37.4	2.39	CSF
F-S20-33/1.0-1.0/9	390	390	-0.46	33.3	91.4	0.71	46.4	38.0	38.0	2.40	CSF
L-S30-50/1.0-1.0/9	457	457	-0.25	50.0	129.5	0.86	106.8	93.0	93.0	1.39	CSF

and Tabuchi et al. [18], as summarised in Table 19. It is shown that the mean $M_{ip,lu}/M_{ip,Pred}$ ratios are 1.36, 1.89, 2.40 and 1.39 for h_0/t_0 ratios of 16.7, 22.2, 33.3 and 50.0, respectively. The three increasing $M_{ip,lu}/M_{ip,Pred}$ ratios, for $h_0/t_0 \leq 33.3$, mean that either the test resistances increase more significantly compared with the predicted design resistances, or the design resistance predictions decrease more pronouncedly with increasing h_0/t_0 ratios, possibly caused by the smaller t_0 values in the assumed bearing length ($B_e = h_1 + 5t_0$) and the buckling reduction factor ($\chi_{0.5}$) linearised against the h_0/t_0 ratio. The relative increase of the test resistance with an increasing h_0/t_0 ratio, for cold-formed hollow section joints, may be due to better performance of RHS joints with thinner chord walls, which have smaller chord corner radii and thus smaller weld gaps at the chord side. However, after an initial increasing effect, a further increase of the h_0/t_0 ratio could have a decreasing effect on the $M_{ip,lu}/M_{ip,Pred}$ ratio. This may be caused by local buckling of the chord sidewall, resulting in more pronounced decrease of the test resistance (e.g., as observed for $h_0/t_0 = 50.0$).

6.3. Effect of steel grades

The material factor (C_f) in Tables 4–5 is adopted from Refs. [37,38] for full-width RHS joints under brace axial compression to consider possible adverse effects of material softening in welding heat-affected zones (HAZ) of high-strength steel and fabrication imperfections. It is noted that reduction of joint strengths can be up to 8% for S960 full-width RHS X- and T-joints under brace axial compression, with maximum reduction of material strengths of 20% in HAZ [33,34]. It is also worth noting that the adopted material factors agree well with those proposed in Ref. [25] for RHS joints subjected to brace axial tension. The proposed material factors in Ref. [25] are 1.0, 0.90 and 0.80 for S500, S700 and S960, respectively, and those adopted in Tables 4–5 are 0.96, 0.90 and 0.83, respectively. However, there are only three specimens (i.e., S500-RX1, S700-RX1 and S960-RX1 in Table 6) using steel grades greater than S460. The N_{lu}/N_{Pred} ratio for the S960 specimen is only 1.05 or 1.18 if the yield stress limit (i.e., $f_y \leq 0.8f_u$) is applied, which is low and may be caused by the small weld size adopted and material softening in HAZ. Thus, more experimental and numerical studies are required for steel grades higher than S460. Furthermore, for the analysed RHS X joints in Table 10, except for specimen S960-RX1, the need for applying the yield stress limit seems to be not apparent, therefore this limit is not imposed in the subsequent design proposals.

6.4. Effect of cross-section class

As shown in Table 4, the design resistance equations for brace failure in RHS X and T joints under brace axial tension are not related to the cross-section class (Class 1–2 or Class 3); however, those for brace in-plane bending and brace out-of-plane bending depend on the cross-section class. Table 5 shows that the cross-section class needs to be considered in the determination of the chord stress ratio (n) and chord sidewall resistances, and the design resistance equations

for brace in-plane bending are directly dependent on the cross-section class. The majority of the compiled RHS X and T joints under brace axial tension in Tables 8–9 have Class 1–3 members, but six RHS X joints (i.e., specimens X6, X7 and X8 [23], specimen S960-RX1 [25], and specimens X4 (45°) and X6 (90°) [26]) used Class 4 cross-sections. The N_{lu}/N_{Pred} ratios of the six specimens, except for specimen S960-RX1, are comparable with those of RHS X and T joints with Class 1–3 cross-sections.

For brace in-plane bending, some of the collated RHS X and T joints (see Tables 13 and 16) have Class 3–4 members, such as the chords of specimens x12ie05, x12i and x12ie2 governed by chord sidewall failure [21], and the chords of specimens C-S20-33/1.0–1.0/9, L-S30-50/1.0–1.0/9 and F-S20-33/1.0–1.0/9 controlled by chord sidewall failure [17,18]. It is demonstrated that the proposed design resistance equations can provide conservative resistance predictions and the corresponding $M_{ip,lu}/M_{ip,Pred}$ ratios are generally higher than 1.4, except for the specimens with weld defects. It is noted that the cross-section of the chord of specimen L-S30-50/1.0–1.0/9 is very slender with $h_0/t_0 = 50.0$, and the corresponding $M_{ip,lu}/M_{ip,Pred}$ ratio is 1.39 (see Table 16), indicating that the design resistance equations for Class 3 cross-sections might also be applicable for some Class 4 cross-sections. For brace out-of-plane bending, the chords of specimens x12oe05, x12o and x12oe2, governed by chord sidewall failure, have Class 3 members (see Table 18), and the corresponding $M_{op,lu}/M_{op,Pred}$ ratios are marginally lower than 1.4. Considering the limited available evidence, it is recommended to apply the proposed design resistance equations to RHS X and T joints with brace and chord cross-section slenderness ratios not exceeding Class 3 and 40, in line with Refs. [37,38,45].

As discussed in Section 5, it is preferred to adopt an elastic analysis (i.e., using the coefficient of 0.33 and W_{el}) for joints where one or all members are Class 3 cross-sections, to be in accordance with the actual load transfer. For brace axial tension, $f_k = f_{y0}$ can be used for steel grades up to and including S700, and for brace out-of-plane bending loading, f_k can be adopted for steel grades up to and including S700. For brace in-plane bending loading, $f_k = f_{y0}$ is suggested for steel grades up to and including S460; however, f_k in combination with an elastic analysis is conservatively recommended for steel grades higher than S460 up to and including S700. This is because test evidence for higher steel grades is limited, and the deformation and rotation capacity of RHS joints in high-strength steel remain unclear. More experimental and numerical investigations are needed to verify the suitability of applying $f_k = f_{y0}$ for high-strength steel RHS X and T joints under brace in-plane bending. It should also be noted that the test evidence is currently not sufficient to give recommendations for RHS joints using steel grades higher than S700, considering that the one S960 RHS X joint under brace axial tension [25] has a low N_{lu}/N_{Pred} ratio of 1.05 (see Table 8).

Table 20

Statistical evaluation for the screened database of 36 RHS X and T joints under brace axial tension.

Specimen	f_{y0} (MPa)	Chord section	f_{y1} (MPa)	Brace section	n	N_{lu} (kN)	N_{BF} (kN)	N_{CSF} (kN)	Predicted Failure	N_{lu}/N_{BF}	N_{lu}/N_{CSF}
X3B	472	Class 1–2	472	Class 1–2	0.60	1368	1057	908	CSF	–	1.51
X4	472	Class 1–2	472	Class 1–2	0.60	1295	1057	908	CSF	–	1.43
X6	425	Class 1–2	425	Class 1–2	0.60	1306	937	804	CSF	–	1.62
X8	482	Class 1–2	482	Class 1–2	0.60	1388	1043	896	CSF	–	1.55
X13	443	Class 1–2	443	Class 1–2	0.60	1602	1417	1191	CSF	–	1.34
X18	468	Class 1–2	468	Class 1–2	0.60	1750	1462	1228	CSF	–	1.43
X19	505	Class 1–2	505	Class 1–2	0.60	1844	1571	1318	CSF	–	1.40
X22	424	Class 1–2	424	Class 1–2	0.60	1720	1251	1063	CSF	–	1.62
X24	499	Class 1–2	499	Class 1–2	0.60	2025	1525	1285	CSF	–	1.58
X26	503	Class 1–2	503	Class 1–2	0.60	1516	1114	957	CSF	–	1.58
X28	511	Class 1–2	511	Class 1–2	0.60	1140	785	673	CSF	–	1.69
X1	516	Class 1–2	516	Class 1–2	0	1262	936	873	CSF	–	1.45
X2	516	Class 1–2	516	Class 1–2	0	1272	929	867	CSF	–	1.47
X4	483	Class 1–2	519	Class 3	0	1069	914	1554	BF	1.17	–
X6	473	Class 4	506	Class 4	0	980	657	715	BF	1.49	–
X7	473	Class 4	479	Class 4	0	1511	1165	1264	BF	1.30	–
X8	473	Class 4	466	Class 4	0	1118	766	717	CSF	–	1.56
X9	483	Class 1–2	483	Class 1–2	0	2075	1666	1553	CSF	–	1.34
X12	451	Class 1–2	451	Class 3	0	820	507	492	CSF	–	1.67
X12C	451	Class 1–2	451	Class 1–2	0	776	518	498	CSF	–	1.56
X1B	516	Class 1–2	516	Class 1–2	0	1335	932	868	CSF	–	1.54
X2B	516	Class 1–2	516	Class 1–2	0	1321	931	868	CSF	–	1.52
X12B	519	Class 3	519	Class 3	0	828	572	555	CSF	–	1.49
CX1RT_420S	529	Class 1–2	529	Class 1–2	0	1031	827	770	CSF	–	1.34
CX1RT_420Rb	488	Class 1–2	488	Class 1–2	0	978	797	739	CSF	–	1.32
CX1-40_420S	547	Class 1–2	547	Class 1–2	0	1129	851	792	CSF	–	1.42
CX1-40_420R	488	Class 1–2	488	Class 1–2	0	1053	797	739	CSF	–	1.43
CX1RT_460V	536	Class 1–2	536	Class 1–2	0	1174	912	840	CSF	–	1.40
CX1-40_460V	536	Class 1–2	536	Class 1–2	0	1246	912	840	CSF	–	1.48
S500-RX1	522	Class 1–2	522	Class 1–2	0	718	522	494	CSF	–	1.45
S700-RX1	725	Class 1–2	725	Class 1–2	0	1154	828	777	CSF	–	1.49
X4 (45°)	438	Class 4	438	Class 4	0	588	426	480	BF	1.38	–
X6 (90°)	449	Class 4	438	Class 4	0	659	591	661	BF	1.11	–
1	317	Class 1–2	317	Class 1–2	–0.94	301	301	210	CSF	–	1.43
1'	317	Class 1–2	317	Class 1–2	–0.92	296	301	215	CSF	–	1.37
7	345	Class 1–2	345	Class 1–2	–0.89	332	354	269	CSF	–	1.23
No. of data										5	31
Mean										1.29	1.47
CoV										0.119	0.073
ϕ										0.99	1.26

7. Reliability analyses for proposed design resistance equations

7.1. Screened database

The collated test results of full-width RHS X and T joints under brace axial tension and brace bending were carefully screened and statistically evaluated, considering the governing predicted failure modes of brace failure and chord sidewall failure. Specimens with reported weld defects and tests with insufficient weld sizes or inadequate weld profiles, which can result in unduly low strength and/or deformation capacity, were excluded in the statistical assessment.

For RHS X and T joints under brace axial tension (see Tables 8–9), the following tests were not included in the screened database:

- (1) B-1 and B-4 by Davies et al. [6], because of weld slag inclusions.
- (2) All tests by Mang et al. [19] because these were reported to fail by weld-related failure modes.
- (3) X3A by Björk [22] due to inadequate weld profile, CX1RT_420R by Tuominen and Björk [24] due to failing at the chord seam weld, and S960-RX1 by Feldmann et al. [25] which had a small weld size to the brace transverse wall.
- (4) 4, 10 and 10' by Wardenier and de Koning [4] because they were governed by chord member failure, and 4' which had an extremely high n value.

For RHS X and T joints under brace in-plane bending (see Tables 13 and 16), the following specimens were excluded in the screened database:

- (1) x12ie05 by Yu [21], which was determined by numerical simulation, but the fracture failure criterion was inadequate.
- (2) 1g by Mang et al. [7], which had an extremely high n value and was governed by chord member failure.
- (3) M-S20-22/1.0–0.67/6 and N-S20-17/1.0–0.5/9 by Kanatani et al. [17], and K-S20-17/1.0–0.5/9 by Tabuchi et al. [18], which had inadequate weld details. C-S20-33/1.0–1.0/9 and F-S20-33/1.0–1.0/9 [17,18] had abnormally high $M_{ip,lu}/M_{ip,Pred}$ ratios.

For RHS X and T joints under brace out-of-plane bending, the specimens analysed by Yu [21] (see Table 18) were compiled, and the values of $M_{op,lu}/M_{op,Pred}$ ratio are comparable with those of N_{lu}/N_{Pred} ratio in Table 8. Therefore, all of these specimens were included for the statistical evaluation.

After screening out the aforementioned specimens, the reduced database for brace axial tension is listed in Table 20, and those for brace in-plane bending and brace out-of-plane bending are shown in Tables 21 and 22, respectively. For brace failure, there remain five specimens for brace axial tension, with a mean value of N_{lu}/N_{BF} ratio of 1.29 and corresponding coefficient of variation (CoV) of 0.119, and three specimens for brace in-plane bending, with a mean value of $M_{ip,lu}/M_{ip,BF}$ ratio of 1.74 and corresponding CoV of 0.197. This indicates that the proposed design resistance equations can provide conservative resistance predictions for brace failure. For chord sidewall failure, there remain 31 specimens for brace axial tension, 20 specimens for brace in-plane bending and eight specimens for brace out-of-plane bending. The corresponding mean values of N_{lu}/N_{CSF}

Table 21

Statistical evaluation for the screened database of 23 RHS X and T joints under brace in-plane bending.

Specimen	f_{y0} (MPa)	Chord section	f_{y1} (MPa)	Brace section	n	$M_{ip,1u}$ (kNm)	$M_{ip,BF}$ (kNm)	$M_{ip,CSF}$ (kNm)	Predicted failure	$M_{ip,1u}/M_{ip,BF}$	$M_{ip,1u}/M_{ip,CSF}$
9a	279	Class 1–2	367	Class 1–2	–0.13	19.0	16.4	15.0	CSF	–	1.27
9b	367	Class 1–2	367	Class 1–2	–0.13	16.5	11.5	10.4	CSF	–	1.59
x10ie05	355	Class 1–2	690	Class 1–2	0	37.1	27.6	27.7	BF	1.35	–
x10ie	355	Class 1–2	690	Class 1–2	0	89.7	92.5	71.0	CSF	–	1.26
x10ie2	355	Class 1–2	690	Class 4	0	259.7	226.2	143.5	CSF	–	1.81
x11i	355	Class 1–2	690	Class 1–2	0	50.0	52.9	36.4	CSF	–	1.37
x11ie2	355	Class 1–2	690	Class 4	0	128.7	132.4	80.3	CSF	–	1.60
x12i	355	Class 3	690	Class 4	0	28.6	21.9	14.8	CSF	–	1.94
x12ie2	355	Class 3	690	Class 4	0	76.5	87.6	51.9	CSF	–	1.47
1a	332	Class 1–2	332	Class 1–2	–0.28	17.1	11.5	10.6	CSF	–	1.61
1b	332	Class 1–2	332	Class 1–2	–0.36	16.5	11.8	10.7	CSF	–	1.55
1c	332	Class 1–2	332	Class 1–2	–0.55	16.3	11.5	10.1	CSF	–	1.61
1d	332	Class 1–2	332	Class 1–2	–0.63	14.3	11.7	10.1	CSF	–	1.41
1e	314	Class 1–2	314	Class 1–2	–0.25	8.6	4.3	5.7	BF	1.98	–
1f	314	Class 1–2	314	Class 1–2	–0.79	9.0	4.7	5.3	BF	1.90	–
M-S20-22/1.0-0.67/6	355	Class 1–2	392	Class 3	–0.44	108.6	74.7	59.7	CSF	–	1.82
M-S20-22/1.0-0.67/9E	355	Class 1–2	392	Class 3	–0.45	112.6	74.7	59.6	CSF	–	1.89
M-S20-22/1.0-0.67/9	355	Class 1–2	392	Class 3	–0.47	116.3	74.7	59.4	CSF	–	1.96
N-S20-17/1.0-0.5/6E	378	Class 1–2	392	Class 3	–0.40	129.5	109.8	95.6	CSF	–	1.35
N-S20-17/1.0-0.5/9E	378	Class 1–2	392	Class 3	–0.40	129.4	109.8	95.6	CSF	–	1.35
L-S30-50/1.0-1.0/9	457	Class 4	457	Class 4	–0.25	129.5	106.8	93.0	CSF	–	1.39
K-S20-17/1.0-0.5/6E	385	Class 1–2	400	Class 3	–0.40	131.9	111.8	97.2	CSF	–	1.36
K-S20-17/1.0-0.5/9E	385	Class 1–2	400	Class 3	–0.40	132.0	111.8	97.2	CSF	–	1.36
									No. of data	3	20
									Mean	1.74	1.55
									CoV	0.197	0.147
									ϕ	1.13	1.12

Table 22

Statistical evaluation for the database of 8 RHS X joints under brace out-of-plane bending.

Specimen	f_{y0} (MPa)	Chord section	f_{y1} (MPa)	Brace section	n	$M_{op,1u}$ (kNm)	$M_{op,BF}$ (kNm)	$M_{op,CSF}$ (kNm)	Predicted failure	$M_{op,1u}/M_{op,CSF}$
x10oe05	355	Class 1–2	690	Class 1–2	0	80.4	82.8	62.1	CSF	1.29
x10oe	355	Class 1–2	690	Class 1–2	0	119.4	148.4	93.4	CSF	1.28
x10oe2	355	Class 1–2	690	Class 4	0	192.5	250.4	147.4	CSF	1.31
x11o	355	Class 1–2	690	Class 1–2	0	59.4	91.9	48.1	CSF	1.24
x11oe2	355	Class 1–2	690	Class 4	0	108.6	164.1	79.2	CSF	1.37
x12oe05	355	Class 3	690	Class 4	0	23.0	29.9	16.6	CSF	1.38
x12o	355	Class 3	690	Class 4	0	37.2	57.4	26.6	CSF	1.40
x12oe2	355	Class 3	690	Class 4	0	62.7	115.3	45.0	CSF	1.39
									No. of data	8
									Mean	1.33
									CoV	0.045
									ϕ	1.21

Table 23Proposed design rules for full-width RHS X and T joints ($\beta = 1.0$) under brace axial tension.

Brace failure	$N_{Rd,BF} = C_{t1} f_{y1} [A_1 - 2(b_1 - b_e)t_1]$
Chord sidewall failure	$N_{Rd,CSF} = C_{t0} f_{y0} t_0 (2h_1 + 10t_0) Q_t \sqrt{\frac{1}{\sin \theta_1}}$
Parameters	<p>1. Brace effective width (b_e) is determined from:</p> $b_e = \frac{10}{b_0/t_0} \frac{f_{y0} t_0}{f_{y1} t_1} b_1 \text{ but } \leq b_1$ <p>2. Brace and chord material factors (C_{t1} and C_{t0}) are taken as:</p> $C_{t1} = 1.1 - 0.1 f_{y1}/355 \text{ but } \leq 1.0$ $C_{t0} = 1.1 - 0.1 f_{y0}/355 \text{ but } \leq 1.0$ <p>3. Chord stress function (Q_t) is taken as:</p> $Q_t = (1 - n)^{0.1} \text{ with } n \text{ in connecting chord face defined by}$ $n = \frac{N_{0,Ed}}{N_{pl,0,Rd}} + \frac{M_{0,Ed}}{M_{pl,0,Rd}} \text{ for Class 1 and 2 chord cross-sections under chord compression stress and for chord cross-sections under chord tension stress; } M_{el,0,Rd} \text{ should be used for Class 3 chord cross-sections}$
Validity range	See Table 26

Table 24Proposed design rules for full-width RHS X and T joints ($\beta = 1.0$) under **brace in-plane bending**.

Brace failure^a	$M_{Rd,BF} = C_{t1} f_{y1} [W_{pl,1} - (b_1 - b_e)(h_1 - t_1)t_1]$ for Class 1 or 2 cross-sections $M_{Rd,BF} = C_{t1} f_{y1} [W_{el,1} - (b_1 - b_e)(h_1 - t_1)t_1]$ for Class 3 cross-sections
Chord sidewall failure^a	$M_{Rd,CSF} = 0.5C_{t0}f_k t_0 (h_1 + 5t_0)^2 Q_f$ for Class 1 or 2 cross-sections $M_{Rd,CSF} = 0.33C_{t0}f_k t_0 (h_1 + 5t_0)^2 Q_f$ for Class 3 cross-sections
Parameters	<p>1. Brace effective width (b_e) is determined from:</p> $b_e = \frac{10}{b_0/t_0} \frac{f_{y0}t_0}{f_{y1}t_1} b_1 \text{ but } \leq b_1$ <p>2. Buckling stress (f_k) is taken as:</p> $f_k = f_{y0} \text{ for } f_{y0} \leq 460 \text{ MPa}$ $f_k = \chi_{0.5} \left(\frac{h_0}{0.5h_1} \right)^{0.15} f_{y0} \text{ but } \leq f_{y0} \text{ and use the design equations for Class 3 cross-sections for } 460 < f_{y0} \leq 700 \text{ MPa}$ <p>3. Buckling reduction factor ($\chi_{0.5}$) is determined by:</p> $\chi_{0.5} = 1.12 - 0.012 \frac{h_0}{t_0} \sqrt{\frac{f_{y0}}{355}}$ <p>Alternatively, $\chi_{0.5}$ value may also be derived according to e.g., EN1993-1-1 [39] or equivalents using the buckling curve c and a non-dimensional slenderness:</p> $\lambda_{0.5} = \frac{1.73 \left(\frac{h_0}{t_0} - 2 \right)}{\pi \sqrt{\frac{E}{f_{y0}}}}$ <p>4. Brace and chord material factors (C_{t1} and C_{t0}) are taken as:</p> $C_{t1} = 1.1 - 0.1f_{y1}/355 \text{ but } \leq 1.0$ $C_{t0} = 1.1 - 0.1f_{y0}/355 \text{ but } \leq 1.0$ <p>5. Chord stress function (Q_f) is taken as:</p> $Q_f = (1 - n)^{0.1} \text{ with } n \text{ in connecting chord face defined by}$ $n = \frac{N_{0,Ed}}{N_{pl,0,Rd}} + \frac{M_{0,Ed}}{M_{pl,0,Rd}} \text{ for Class 1 and 2 chord cross-sections under chord compression stress and for chord cross-sections under chord tension stress; } M_{el,0,Rd} \text{ should be used for Class 3 chord cross-sections}$
Validity range	See Table 26

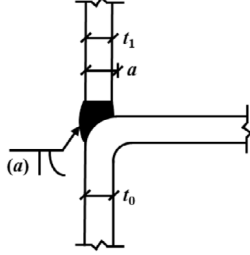
^aIf one of the cross-sections of either the brace or chord is classified as Class 3, the Class 3 design resistance is used.

Table 25Proposed design rules for full-width RHS X and T joints ($\beta = 1.0$) under **brace out-of-plane bending**.

Brace failure^a	$M_{Rd,BF} = C_{t1} f_{y1} [W_{pl,1} - 0.5(b_1 - b_e)^2 t_1]$ for Class 1 or 2 cross-sections $M_{Rd,BF} = C_{t1} f_{y1} [W_{el,1} - 0.33(b_1 - b_e)^2 t_1]$ for Class 3 cross-sections
Chord sidewall failure	$M_{Rd,CSF} = C_{t0} f_k t_0 (h_1 + 5t_0)(b_1 - t_0) Q_f$
Parameters	<p>1. Brace effective width (b_e) is determined from:</p> $b_e = \frac{10}{b_0/t_0} \frac{f_{y0}t_0}{f_{y1}t_1} b_1 \text{ but } \leq b_1$ <p>2. Buckling stress (f_k) is taken as:</p> $f_k = \chi_{0.5} \left(\frac{h_0}{h_1} \right)^{0.15} f_{y0} \text{ but } \leq f_{y0}$ <p>3. Buckling reduction factor ($\chi_{0.5}$) is determined by:</p> $\chi_{0.5} = 1.12 - 0.012 \frac{h_0}{t_0} \sqrt{\frac{f_{y0}}{355}}$ <p>Alternatively, $\chi_{0.5}$ value may also be derived according to e.g., EN1993-1-1 [39] or equivalents using the buckling curve c and a non-dimensional slenderness:</p> $\lambda_{0.5} = \frac{1.73 \left(\frac{h_0}{t_0} - 2 \right)}{\pi \sqrt{\frac{E}{f_{y0}}}}$ <p>4. Brace and chord material factors (C_{t1} and C_{t0}) are taken as:</p> $C_{t1} = 1.1 - 0.1f_{y1}/355 \text{ but } \leq 1.0$ $C_{t0} = 1.1 - 0.1f_{y0}/355 \text{ but } \leq 1.0$ <p>5. Chord stress function (Q_f) is taken as:</p> $Q_f = (1 - n)^{0.1} \text{ with } n \text{ in connecting chord face defined by}$ $n = \frac{N_{0,Ed}}{N_{pl,0,Rd}} + \frac{M_{0,Ed}}{M_{pl,0,Rd}} \text{ for Class 1 and 2 chord cross-sections under chord compression stress and for chord cross-sections under chord tension stress; } M_{el,0,Rd} \text{ should be used for Class 3 chord cross-sections}$
Validity range	See Table 26

^aIf one of the cross-sections of either the brace or chord is classified as Class 3, the Class 3 design resistance is used.

Table 26
Range of validity of the proposed design rules for full-width RHS X and T joints.

Welding	Weld effective throats are to develop the full capacity of the connected member wall, using fillet or groove welds (or a combination thereof) to the brace transverse walls, and groove welds to the brace longitudinal walls at the chord corners. Prequalified groove welds (see the figure below) are to comply with the relevant welding standard, with brace edge preparation or backing, as required.
 <p>(a)</p>	
Steel grade	Up to and including S700 or equivalent
Cross-section limit	b_0/t_0 , h_0/t_0 , b_1/t_1 and $h_1/t_1 \leq 40$; brace and chord cross-sections to be Class 1-3, the limits for which can be determined in line with relevant design codes, such as EN 1993-1-1 [39]

ratio, $M_{ip,u}/M_{ip,CSF}$ ratio and $M_{op,u}/M_{op,CSF}$ ratio are 1.47, 1.55 and 1.33 with CoVs of 0.073, 0.147 and 0.045, respectively. Thus, the proposed design resistance equations are conservative for chord sidewall failure.

7.2. Reliability analyses

Similar to the loading case of brace axial compression examined in Refs. [37,38], simplified reliability analyses have been carried out, considering the non-ductile nature of the failure modes. Commentary Section B3.1 to AISC 360-16 [48] recommends a reliability index of 4.0 for non-ductile connectors (bolts and welds) or brittle elements. Eq. (1) from Ravindra and Galambos [49] can then be used to obtain the required resistance factors. It is noted that Eq. (1) neglects the beneficial overall effects of including statistical parameters for geometrical and material properties (thus making it conservative), and probability distributions associated with the loading are not considered.

$$\phi = (\text{Mean}) e^{(-0.55)(4.0)(\text{CoV})} \quad (1)$$

Tables 20–22 summarise the resulting resistance factors (ϕ) to be applied to the design resistance equations for brace failure and chord sidewall failure. It is shown that, for brace failure, the obtained ϕ values are 0.99 and 1.13 for brace axial tension and brace in-plane bending. For chord sidewall failure, the ϕ values are 1.26, 1.12 and 1.21 for brace axial tension, brace in-plane bending and brace out-of-plane bending, respectively. As ϕ is intended as a reduction factor (≤ 1.0), a unified resistance factor of unity is recommended to be applied to the design resistance equations for both the brace failure and chord sidewall failure limit states for all joint types considered. Note that the resistance factor of unity herein can be viewed as an adjustment factor that needs to be applied to the design resistance equations being evaluated. Thus, it is confirmed that the proposed design resistances can provide adequate reliability, as-is. It should be noted that, although a conservative unified resistance factor of unity is recommended for all the loading cases, the effects of secondary bending moments are not considered in the design rules proposed in this study.

8. Proposed design rules

Based on the foregoing analyses, it is proposed to adopt, for brace failure and chord sidewall failure in RHS X and T joints, the design rules summarised in Tables 23–25 and the corresponding validity range is given in Table 26.

9. Conclusions

This paper presents an investigation into the pertinent limit states for full-width rectangular hollow section (RHS) X and T joints under brace axial tension, brace in-plane bending and brace out-of-plane bending. Current codified design rules and their limitations, for the design of full-width RHS joints, are discussed. Design resistance equations for the two governing limit states in full-width RHS joints – brace failure and chord sidewall failure – are proposed. Experimental and numerical results for full-width RHS joints are collated from the literature, covering a wide range of geometrical parameters, steel grades ranging from S235 to S960, varying weld details, and loading cases of brace axial tension, brace in-plane bending and brace out-of-plane bending. The compiled test database is screened and then used to evaluate the performance of full-width RHS joints and the proposed design resistance equations. The conclusions are summarised as follows:

- (1) The effects of weld details on joint strength and deformation capacity are significant. Sufficient weld sizes, adequate weld profiles and brace end preparations, as required, should be adopted for welding at the brace–chord junction.
- (2) Welding guidance and user-friendly design rules are proposed for brace failure and chord sidewall failure in full-width RHS joints subjected to brace axial tension, brace in-plane bending and brace out-of-plane bending.
- (3) The proposed design resistance equations provide conservative and reliable resistance predictions.
- (4) The design proposals have been verified to be suitable for Class 1–3 cross-sections, as stipulated in EN 1993-1-1 [39], which relax the Class 1–2 limitation on cross-section class in current design codes and guides.

CRediT authorship contribution statement

Xiaoyi Lan: Writing – original draft, Investigation. **Jaap Wardenier:** Writing – review & editing, Investigation. **Jeffrey A. Packer:** Writing – review & editing, Investigation.

Declaration of competing interest

The authors declare that they have no known competing financial interests or personal relationships that could have appeared to influence the work reported in this paper.

Data availability

Data will be made available on request.

References

- [1] Stewarts, Lloyds, The local crushing strength of RHS junction, in: Report C/E 64/65/1, UK, 1965.
- [2] P. Bettzieche, Konstruktive Gestaltung Von Knotenpunkten Aus Vierkanthohlprofilen, Studienhefte zum Fertigbau, Vulkan Verlag, Essen, Germany, 1969.
- [3] W. Eastwood, C. Osgerby, A.A. Wood, B.L. Mee, An Experimental Investigation of Joints in Rectangular Hollow Sections, University of Sheffield, Sheffield, UK, 1970.
- [4] J. Wardenier, Koning C.H.N. de, Static tensile tests on T-joints in structural hollow sections - determination of the influence of weld method and type of material, in: Stevin Report 6-74-7, Delft, Delft University of Technology, The Netherlands, 1974.
- [5] J. Barentse, Investigation into the static strength of welded T-joints made of rectangular hollow sections, in: Stevin Reports 6-76-23 and 6-77-7, Delft University of Technology, The Netherlands, 1977.
- [6] G. Davies, J. Wardenier, P. Stolle, The effective width of branch cross-walls for RR cross joints in tension, in: Stevin Report 6-81-7, Delft, Delft University of Technology, The Netherlands, 1981.
- [7] F. Mang, O. Bučak, F. Wolfmüller, Bemessungsverfahren Für T-Knoten Aus Rechteck-Hohlprofilen. Projekt 82, University of Karlsruhe, Germany, 1981.
- [8] J. Wardenier, G. Davies, The strength of predominantly statically loaded joints with a square or rectangular hollow section chord. IIW Doc. XV-462-81, 1981.
- [9] J. Wardenier, Hollow Section Joints, Delft University Press, The Netherlands, 1982.
- [10] Eurocode 3 (EC3), Design of steel structures-Part 1-8: Design of joints, EN 1993-1-8, European Committee for Standardization, CEN, Brussels, Belgium, 2005.
- [11] Static design procedure for welded hollow-section joints-Recommendations, ISO/FDIS 14346, International Standardization Organization, ISO, Geneva, Switzerland, 2013.
- [12] J.A. Packer, J. Wardenier, Y. Kurobane, D. Dutta, N. Yeomans, Design Guide for Rectangular Hollow Section (RHS) Joints under Predominantly Static Loading, 1st Ed. CIDECT, Verlag TUV Rheinland, Cologne, Germany, 1992.
- [13] J.A. Packer, J. Wardenier, X.L. Zhao, G.J. van der Vegte, Y. Kurobane, Design Guide for Rectangular Hollow Section (RHS) Joints under Predominantly Static Loading, 2nd Ed. CIDECT, Geneva, Switzerland, 2009.
- [14] Design recommendations for hollow section joints-Predominantly statically loaded, 1st Ed. International Institute of Welding (IIW), Subcommission XV-E, Rev. IIW Doc. XV-491-81, 1981.
- [15] Design recommendations for hollow section joints-Predominantly statically loaded, 2nd Ed. International Institute of Welding (IIW), Subcommission XV-E, IIW Doc. XV-701-89, 1989.
- [16] Static design procedure for welded hollow section joints-Recommendations, 3rd Ed. International Institute of Welding (IIW), Subcommission XV-E, IIW Doc. XV-1402-12, 2012.
- [17] H. Kanatani, K. Fujiwara, T. Kamba, Bending Tests on T-Joints of RHS Chord and RHS Branch, CIDECT Final Report, 5AF/2-82/2, 1982.
- [18] M. Tabuchi, H. Kanatani, T. Kamba, The local strength of welded RHS T-joints subjected to bending moment, IIW-Doc. XV-563-84, 1984.
- [19] F. Mang, O. Bučak, F. Wolfmüller, The development of recommendations for the design of welded joints between steel structural hollow sections (T- and X-joints) - German Part for Final report ECSC, CIDECT programme 5AD-84-12, 1983.
- [20] J.A. Packer, Web crippling of rectangular hollow sections, J. Struct. Eng. 110 (10) (1984) 2357–2373.
- [21] Y. Yu, The Static Strength of Uniplanar and Multiplanar Connections in Rectangular Hollow Sections, (Ph.D. thesis), Delft University Press, Delft, The Netherlands, 1997.
- [22] T. Björk, Ductility and Ultimate Strength of Cold-Formed Rectangular Hollow Section Joints At Sub-Zero Temperatures (Thesis), Lappeenranta University of Technology, Lappeenranta, Finland, 2005.
- [23] T. Björk, H. Saastamoinen, Capacity of CFRHS X Joints Made of Double-Grade S420 Steel. Proceedings of 14th International Symposium on Tubular Structures, Taylor & Francis, Group, London, U.K., 2012.
- [24] N. Tuominen, T. Björk, Capacity of RHS-Joints Made of High Strength Steels, CIDECT Report 5BZ, Lappeenranta University of Technology, Finland, 2016.
- [25] M. Feldmann, N. Schillo, S. Schaffrath, K. Virdi, T. Björk, N. Tuominen, M. Veljkovic, M. Pavlovic, P. Manoleas, M. Heinisuo, K. Mela, P. Ongelin, I. Valkonen, J. Minkinen, J. Erkkilä, E. Pétursson, M. Clarin, A. Seyr, L. Horváth, B. Kövesdi, P. Turán, B. Somodi, Rules on High Strength Steel, Publications Office of the European Union, Luxembourg, 2016.
- [26] J. Becque, T. Wilkinson, The capacity of grade C450 cold-formed rectangular hollow section T- and X-connections: an experimental investigation, J. Constr. Steel Res. 133 (2017) 345–359.
- [27] J.H. Kim, C.H. Lee, S.H. Kim, K.H. Han, Experimental and analytical study of high-strength steel RHS X-joints under axial compression, J. Struct. Eng. 145 (12) (2019) 04019148.
- [28] S.H. Kim, C.H. Lee, Chord sidewall failure of RHS X-joints in compression and associated design recommendations, J. Struct. Eng. 147 (8) (2021) 04021111.
- [29] M. Pandey, B. Young, Structural performance of cold-formed high strength steel tubular X-joints under brace axial compression, Eng. Struct. 208 (2020) 109768.
- [30] M. Pandey, B. Young, Compression capacities of cold-formed high strength steel tubular T-joints, J. Constr. Steel Res. 162 (2019) 105650.
- [31] M. Pandey, B. Young, Tests of cold-formed high strength steel tubular T-joints, Thin Wall. Struct. 143 (2019) 106200.
- [32] M. Pandey, B. Young, Static resistances of cold-formed high strength steel tubular non-90° X-joints, Eng. Struct. 239 (2021) 112064.
- [33] X.Y. Lan, T.M. Chan, B. Young, Structural behaviour and design of high strength steel RHS X-joints, Eng. Struct. 200 (2019) 109494.
- [34] X.Y. Lan, T.M. Chan, B. Young, Testing, finite element analysis and design of high strength steel RHS T-joints, Eng. Struct. 227 (2020) 111184.
- [35] J. Kuhn, J.A. Packer, Y.J. Fan, RHS webs under transverse compression, Can. J. Civil Eng. 46 (9) (2019) 810–827.
- [36] J. Becque, S. Cheng, Sidewall buckling of equal-width RHS truss X-joints, J. Struct. Eng. 143 (2) (2016) 04016179.
- [37] J. Wardenier, X.Y. Lan, J.A. Packer, Evaluation of design methods for chord sidewall failure in RHS joints using steel grades up to S960 – State of the art, IIW Doc. XV-E-489-20, 2020.
- [38] X. Lan, J. Wardenier, J.A. Packer, Design of chord sidewall failure in RHS joints using steel grades up to S960, Thin Wall. Struct. 163 (2021) 107605.
- [39] Eurocode 3 (EC3), Design of steel structures-Part 1-1: General rules and rules for buildings, EN 1993-1-1, European Committee for Standardization, CEN, Brussels, Belgium, 2005.
- [40] Eurocode 3 (EC3), Design of steel structures-Part 1-12: General-high strength steels, EN 1993-1-12, European Committee for Standardization, CEN, Brussels, Belgium, 2007.
- [41] J.C. Platt, Sidewall behaviour in full-width rectangular hollow section joints, (Ph.D. thesis), University of Nottingham, Nottingham, U.K., 1984.
- [42] G. Davies, K. Roodbaraky, The effect of angle on the strength of RHS joints, in: Proceedings of the International Meeting on Safety Criteria in Design of Tubular Structures, Tokyo, Japan, 1987.
- [43] Hot finished structural hollow sections of non-alloy and fine grain steels-Part 2: Tolerances, dimensions and sectional properties, EN 10210-2, European Committee for Standardization, CEN, Brussels, Belgium, 2006.
- [44] Cold formed structural hollow sections of non-alloy and fine grain steels-Part 2: Tolerances, dimensions and sectional properties, EN 10219-2, European Committee for Standardization, CEN, Brussels, Belgium, 2006.
- [45] J. Wardenier, X.Y. Lan, J.A. Packer, Re-analysis of full-width RHS T- and X-joints under brace axial tension and brace in-plane bending. IIW Doc. XV-E-500-21, 2021.
- [46] C.H.N. de Koning, J. Wardenier, The static strength of welded joints between structural hollow sections or between structural hollow sections and H-sections part 2: Joints between rectangular hollow sections, Stevin report 9-84-19, Delft, The Netherlands, 1984.
- [47] Structural welding code-steel, AWS D1.1/D1.1M, 24th Ed. American Welding Society (AWS), Florida, U.S.A., 2020.
- [48] Specification for structural steel buildings, American Institute of Steel Construction (AISC), ANSI/AISC 360-16, Chicago, U.S.A., 2016.
- [49] M.K. Ravindra, T.V. Galambos, Load and resistance factor design for steel, J. Struct. Div. 104 (ST9) (1978) 1337–1353.